Imaging of Headache

4

Maja Ukmar, Roberta Pozzi Mucelli,
Irene Zorzenon, and Maria Assunta Cova

4.1 Introduction

Headache is one of the most frequent reported symptoms in neurological clinical practice. Nevertheless only a relatively small group of patients needs neuroimaging in order to confirm the diagnosis. Mainly the cause and the diagnosis are based on the clinical history and neurological examination and are focused on symptoms or signs which prompt further diagnostic testing. Neuroimaging usually is not required in the setting of primary headaches, although it can show same pathological features, but it is important in the evaluation of the secondary ones in order to exclude potentially curable headaches [1].

4.2 Imaging Modalities

Imaging modalities in the diagnostic algorithm of headache are computed tomography (CT), magnetic resonance (MR), and angiography.

CT is the preferred technique in the emergency setting, usually to rule out an intracranial mass or hemorrhage. Evaluation with bone windows is useful to exclude bone lesions or infectious disease of paranasal sinuses. In addition, in the presence of hemorrhage, it could be useful to perform a CT angiography (CTA) to evaluate the presence of aneurysms or vascular malformations. A CT scan after contrast media administration, in venous phase, could also rule out venous cerebral thrombosis. More recently CT perfusion, performed during contrast media administration and dynamic continuous scan acquisition of a brain volume (whole brain with newest CT), is applied in many centers in the evaluation of patients with acute onset of neurological deficit in suspected acute stroke. CT perfusion may help in the differentiation between acute stroke and migrainous aura.

MR is the technique of choice in the evaluation of patients with headache. The technique varies depending on different clinical issues. Whereas in the study of primary headache contrast media administration is not needed, contrarily it is useful in the evaluation of secondary headaches. In primary headache the examination consists mainly of T1, T2, and FLAIR imaging. A MR angiography (MRA) without contrast

Electronic Supplementary Material The online version of this chapter (https://doi.org/10.1007/978-3-319-99822-0_4) contains supplementary material, which is available to authorized users.

M. Ukmar (✉)
SC (UCO) Radiologia Diagnostica e Interventistica, Azienda Sanitaria Universitaria Integrata di Trieste (ASUITS), Trieste, Italy
e-mail: maja.ukmar@asuits.sanita.fvg.it

R. Pozzi Mucelli · I. Zorzenon · M. A. Cova
University of Trieste, Department of Radiology, Cattinara Hospital, Trieste, Italy
e-mail: m.cova@fmc.units.it

M. A. Cova, F. Stacul (eds.), *Pain Imaging*, https://doi.org/10.1007/978-3-319-99822-0_4

media could be added to exclude aneurysms. In case of suspected intracranial occlusion or stenosis or in the presence of coils, an MRA with contrast media is more accurate. Considering secondary headaches, several sequences could be added to the standard protocol, including GE T2 or SWI sequences and diffusion-weighted (DWI) sequences, and in most of the cases, contrast media should be administrated. In particular the administration of contrast media is mandatory if there is a suspect of meningeal pathology, in case of neoplasms or, in skull base, orbital and rhinogenic causes of headache. In case of hydrocephalus, a phase-contrast sequence could be applied to evaluate cerebrospinal fluid dynamics.

Digital subtraction angiography (DSA) is of value in vascular pathology both as a diagnostic and therapeutic tool.

4.3 Imaging Findings

4.3.1 Primary Headaches

Primary headaches are those where there is no underlying cause identifiable and where the diagnosis is arrived at through detailed history and pattern recognition. Approximately 90% of headaches are of the primary type. Such headaches mainly include tension headache, cluster headache, trigeminal autonomic cephalgias, and migraine.

4.3.1.1 Migraine

Migraine is a common neurological disorder, characterized by paroxysmal attacks of typically unilateral throbbing headache accompanied by nausea, photophobia, and phonophobia that occur with or without aura [2]. Around 25% of people with migraine present transient and reversible neurological symptoms that resolve before the onset of headache (migraine aura). Once the aura is resolved, headache might be mild or even absent. The most frequent type of aura is characterized by visual symptoms with fortification spectra or scintillating scotoma. A subset of migraine attacks may manifest with acute neurologic symptoms that can also be found in acute stroke. Sensory aura is less prevalent and almost always accompanied by visual symptoms [3]. The incidence of migraine attacks varies considerably between individuals; some have several attacks a month, but others have less than a month. In particular attacks of migraine with aura present with a lower frequency, ranging from one to two episodes in a year to one or more attacks in a month [4].

The diagnosis of migraine is based on anamnestic and clinical data; however, substantial problems may arise in the acute phase because accurate information is often incomplete or difficult to obtain [5], especially in those patients that clinically mimic an ischemic stroke. Distinguishing between migrainous aura, cerebral ischemia, and Todd paralysis following a seizure may be difficult, but accurate differential diagnosis is mandatory for a correct treatment.

The role of imaging and specifically of conventional MRI is still debated. The association of migraine phenomena with neuroimaging abnormalities, as demonstrated by CT and MRI, has been the subject of much debate [6].

Possible MRI findings, especially in patients with migraine with aura (MA), are supratentorial, but also subcortical deep white matter lesions (Fig. 4.1), silent posterior circulation territory infarcts, and infratentorial T2-hyperintense lesions [7] (Fig. 4.2). Lesions most frequently described in migraine patients are silent infarct-like lesions with the aspect of white matter T2 or FLAIR hyperintensities at MRI [8], but white matter hyperintensities can also be seen in apparently healthy people [9]. In the most important recent study, the CAMERA analysis (Cerebral Abnormalities in Migraine, an Epidemiological Risk Analysis), that analyzed a total of 295 patients, 161 affected by MA, the authors detected a significant incidence of silent brain infarction in the posterior territory, the majority located in cerebellum and more pronounced in patients with MA (8%). Females with migraine also presented deep white matter lesions, with a higher incidence in patients with higher attack frequency [10].

In the study of Uggetti et al., their results are in opposition with all previous studies, as they

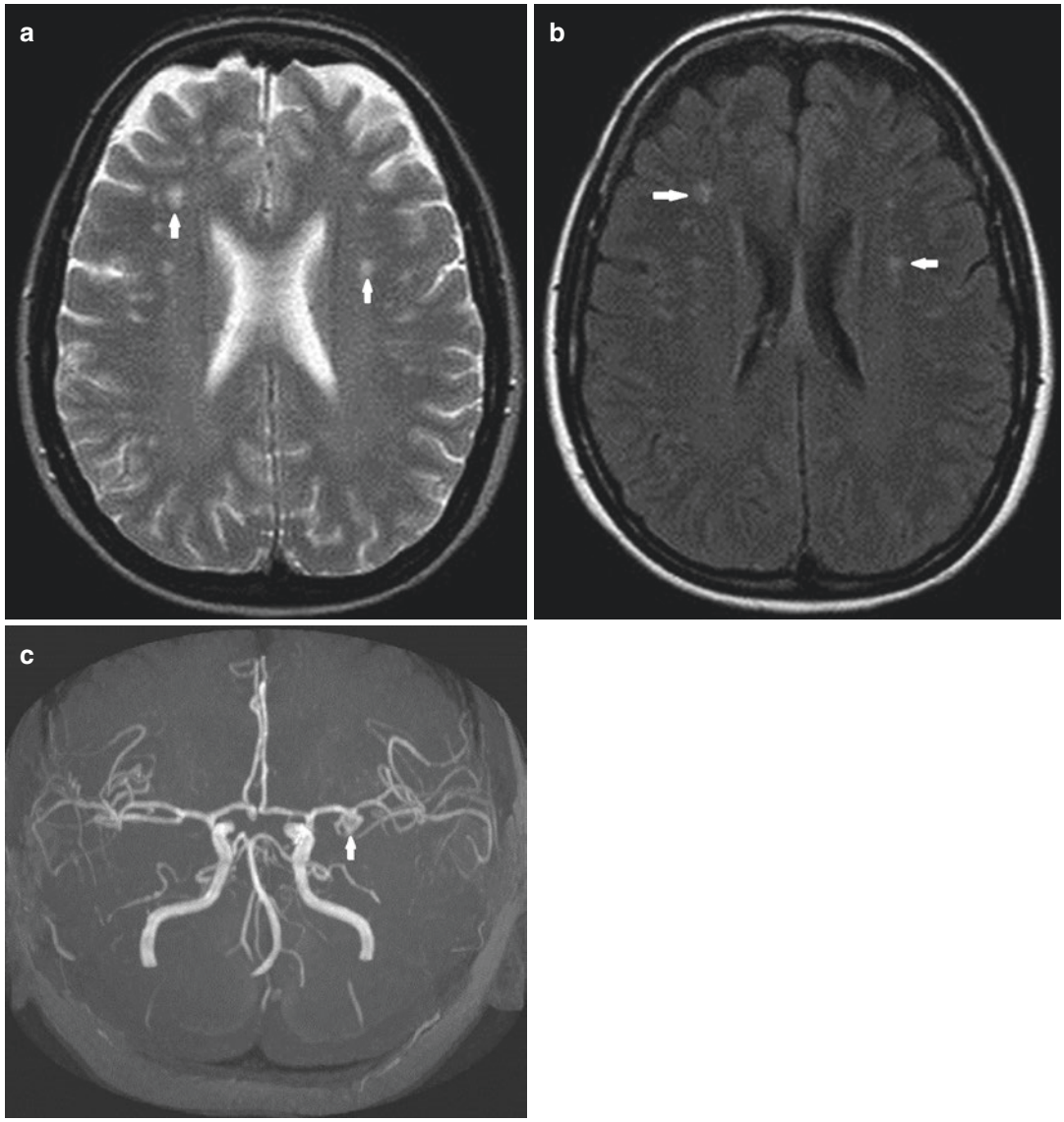

Fig. 4.1 Patient with migraine and aura. Axial SE T2-weighted (**a**) and FLAIR (**b**) sequences show supratentorial white matter hyperintensities. Incidental aneurysms were found on MRA (**c**) at the middle cerebral artery bifurcation and anterior communicating artery

did not find a statistically significant difference in incidence of white matter hyperintensities between patients with MA and controls [11].

Some authors report reversible splenial lesions of the corpus callosum in patients with migraine with aura [12].

Functional neuroimaging of patients with headache is useful to study the pathophysiology rather than for diagnostic purposes. To understand the functional imaging possibilities in headaches, it is necessary to remember how pain structures participate in painful conditions other than headache. In migraine with aura the primary event occurs in the cortex and, including hypothalamus and thalamus, it finishes in the cortex, manifesting pain. In migraine without aura, brain stem findings suggest a dysfunctional pain system [13].

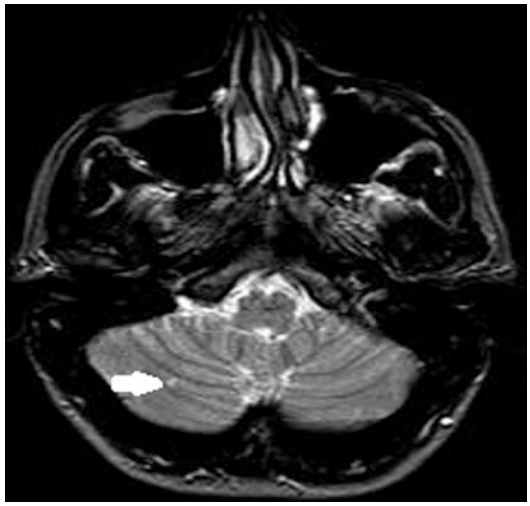

Fig. 4.2 Patient with migraine and aura. Axial SE T2-weighted image: hyperintense specific lesion in the right cerebellum

MR imaging has demonstrated that migrainous aura may be associated with perfusion abnormalities (CBF measurements). Usually, there is hypoperfusion in more than one vascular territory during the migrainous aura, lasting for a few hours (~4), which holds the greatest potential to differentiate migraine from stroke, where hypoperfusion is usually limited to a single vascular territory. A possible differential diagnosis for this pattern of hypoperfusion is severe stenosis of the extracranial vessels; however, this can be assessed by MRA of the extracranial vessels. Some published studies report hyperperfusion; however, this mainly occurs during the headache stage, 6–24 h after the onset of symptoms [14–19]. In literature an occipital predominance of vasoconstriction during the aura is reported [20].

Cerebral perfusion changes during migraine with aura have been described also by BOLD functional MRI studies. In the typical visual aura of migraine, functional MRI has revealed multiple neurovascular events in the occipital cortex, resuming the cortical spreading depression (CSD):

1. An initial hyperemia lasting 3.0–4.5 min, spreading at a rate of 3.5 mm per min.
2. Followed by mild hypoperfusion lasting 1–2 h.
3. An attenuated response to visual activation.
4. Like CSD, in migraine aura, the first affected area is the first to recover [13].

Resnick et al. [21] described reversible changes located in the right parieto-occipital cortex on DWI images in a patient with acute onset of headache. The presence of positive DWI images, with the absence of low apparent diffusion coefficient value, could be in accordance with focal prolonged hyperperfusion associated with vasogenic leakage.

Cerebral perfusion abnormalities may be studied also with CT perfusion; early studies of migraine with aura reveal regional CBF changes of focal hyperemia and spreading oligemia from posterior brain regions. The pathophysiology of the CBF during the acute migraine aura phase and into the period post-headache remains unclear. In the work of Shah et al. [22], they describe the transition from the initial phase of stroke-like symptoms (aura) to an asymptomatic stage, using noninvasive perfusion techniques. There is initial hypoperfusion of the entire left cerebral hemisphere, and the resolution of stroke-like symptoms in 72 h correlates with hyperperfusion and corresponds to decreased MTT and elevated CBF. It is proposed that a "metabolic burnout" leads to possible vasodilation, as there is a gradual increase in CBF (hyperperfusion) seen within the entire left hemisphere. Prior studies from case reports reveal cortical hyperperfusion on the day of migraine aura that carries on until as late as day 14 [23]. There was no documentation of initial hypoperfusion that then resulted in hyperperfusion in any prior case [23]. Perhaps the prolonged and severe symptoms of their case indicate a higher chance of CBF changes occurring as a two-phase process, or possibly other studies have missed the critical moments when such a two-phase process can be imaged. Despite the findings in the literature, in some of our cases (unpublished data) no perfusion defects could be demonstrated.

Noninvasive perfusion techniques allow identifying areas of acute cerebral ischemia and

infarction to assist in determination of the need for thrombolysis with tissue plasminogen activator (tPA). Advanced imaging techniques can be expected to show differentiation between migraine and stroke.

Hemiplegic Migraine

Familial (FHM) and sporadic hemiplegic migraine (SHM) are subtypes of migraine characterized by transient motor weakness during the aura phase and caused by mutations in CACNA1A, ATP1A2, or SCN1A. Its incidence is of 0.01% [24], with the familial and sporadic types occurring with equal frequency.

The pathogenesis of hemiplegic migraine is not well established; however, it is hypothesized that it arises from a wave of neuronal excitation in the gray matter that spreads across the cerebral cortex [25].

The diagnosis of hemiplegic migraine is made clinically in accordance with international guidelines [2]. Hallmark symptoms are intermittent episodes of motor weakness that spontaneously settle over time ranging from hours to weeks.

Neuroimaging in acute attacks of hemiplegic migraine is often normal. However, imaging may reveal cerebral cortical hyperintensity and edema [26, 27] contralateral to the hemiparesis. These abnormalities seen on imaging often resolve within weeks to months after an attack.

Repeated ictal and postictal neuroimaging revealed cytotoxic edema during attacks leading to brain atrophy which halted after cessation of severe HM attacks [28]. A complication of this type of migraine is a migrainous infarction (Fig. 4.3).

Retinal Migraine

Retinal migraine is a rare entity characterized by headache associated with transient monocular visual disturbances. While fully reversible monocular phenomena and normal ophthalmological examination between the attacks are the hallmark of retinal migraine according to the International Headache Society (IHS) classification [2], an association with persistent monocular visual loss and abnormal ophthalmological findings has been reported. Recurrent attacks of retinal migraine may weaken the optic nerve, with a final migraine attack that provokes a permanent visual loss, caused by a threshold rupture of the reduced functional reserve. Vasoconstriction as a potential cause for permanent defects in migraine may be supported by MRI angiography.

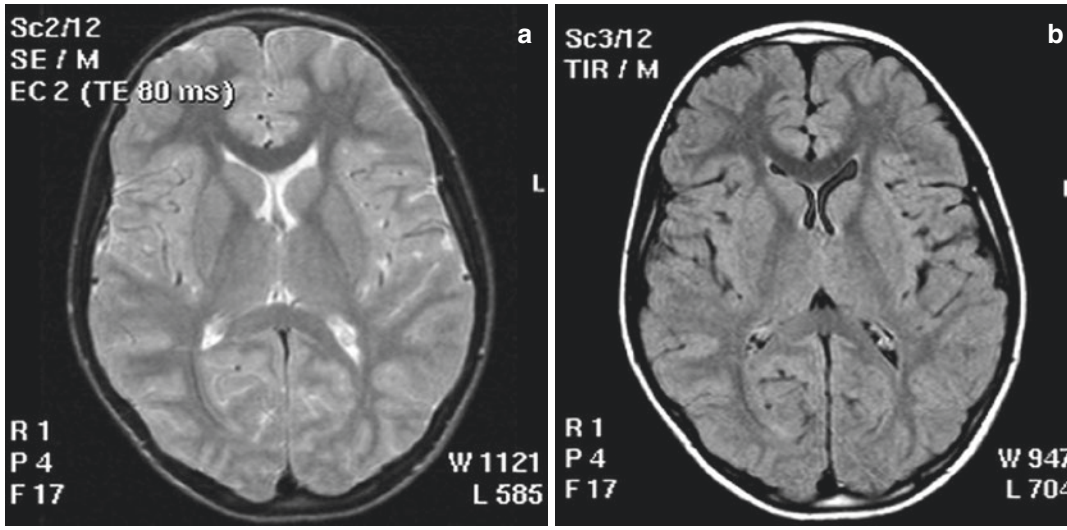

Fig. 4.3 Hemiplegic migraine. Routine MRI exam: Axial SE T2W image (**a**), FLAIR (**b**), and MR angiography (**c**) show no pathologic features. Follow-up MR exam during prolonged left hemiplegia: SE T2W image (**d**), FLAIR (**e**), and DWI (**f**) show acute ischemic stroke in the right thalamus and posterior arm of internal capsule

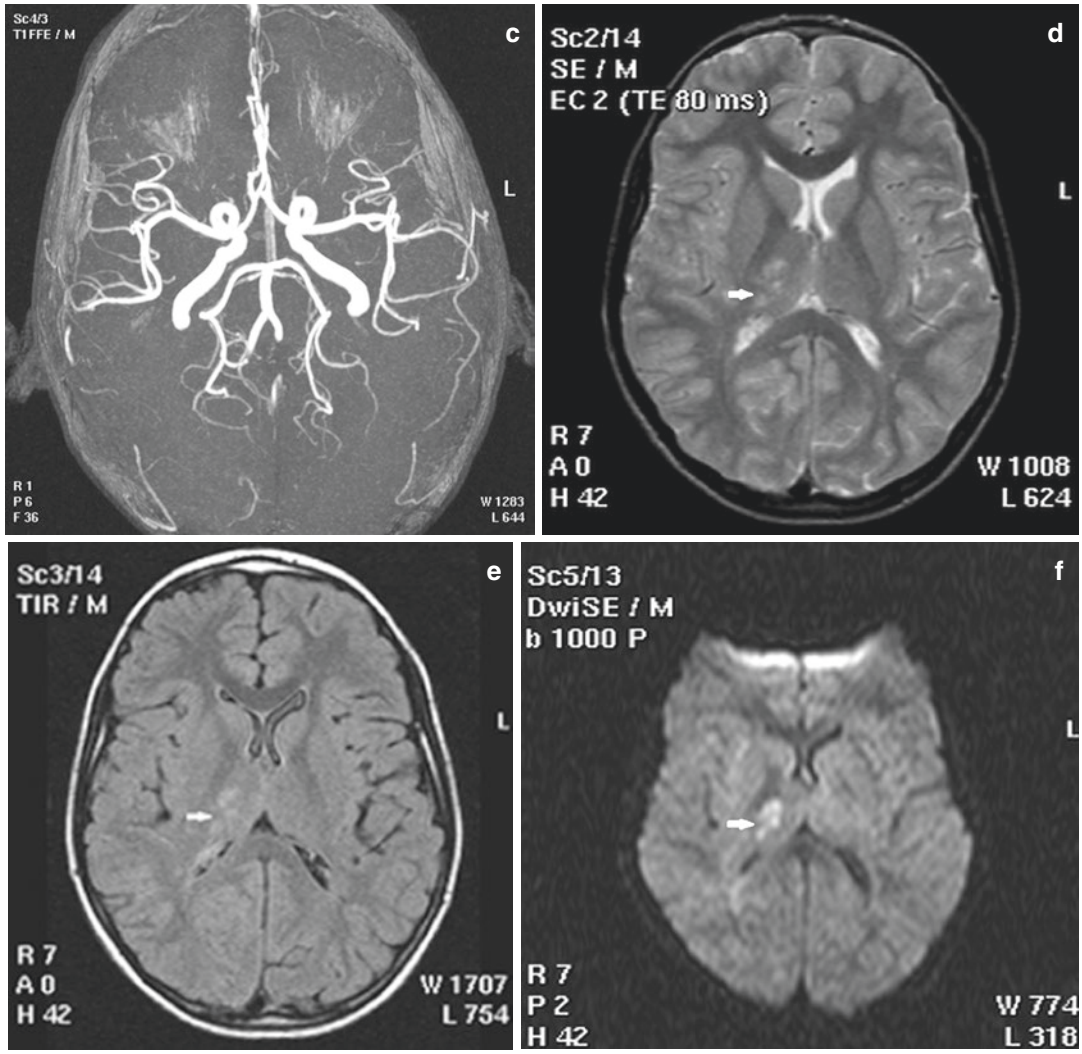

Fig. 4.3 (continued)

MRI, through STIR T2 sequences, may also prove signal alteration of the optic nerve involved, associated with slight bilateral distension of the perioptic subarachnoid spaces. Also at 6 days and 2 months follow-up, a slight pallor and minimal atrophy of the optic disk involved compared to the ipsilateral may be identified [29].

Chronic Migraine

Chronic migraine (CM) usually evolves slowly from episodic migraine (EM) and approximately 2.5% of episodic migraineurs transition to CM each year [30]. Risk factors for chronification include high headache frequency and overuse of acute headache medications among others such as obesity, low educational level, or female sex [31].

The conventional MR patterns are the same as those in episodic migraine. Moreover CM patients show alterations in gray matter volume (GMV) compared to matched healthy controls when analyzed with voxel-based morphometry (VBM). In whole brain analysis testing at a significant threshold of $p < 0.05$ (FEW-corrected), a cluster of GMV increase has been observed with a peak maximum in the amygdala and an

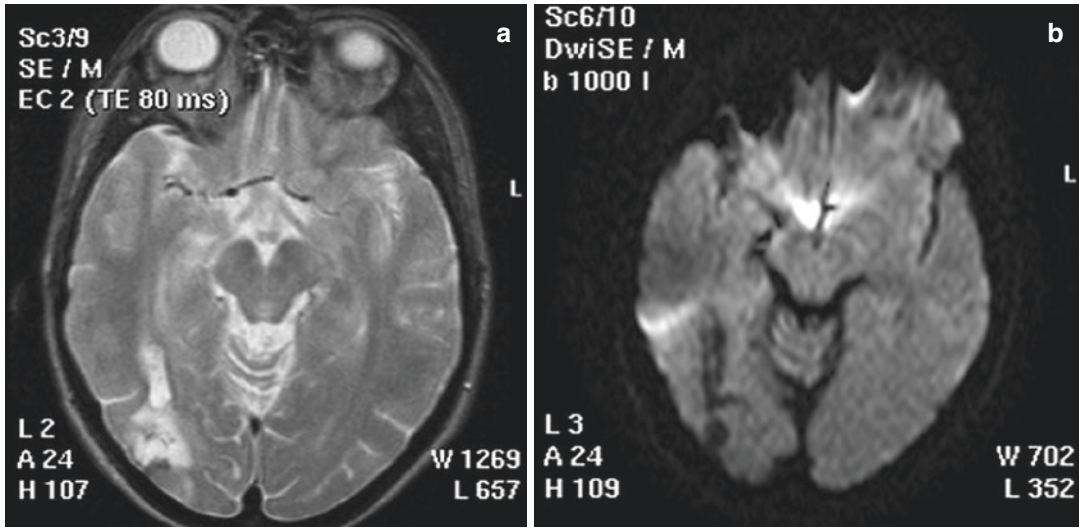

Fig. 4.4 Migrainous infarction. Axial SE T2-weighted image (**a**) and DWI (**b**). Chronic ischemic stroke in right temporal-occipital lobe in a patient with migraine

extension into the putamen [32], which are regions involved in pain perception and processing, but also in affective and cognitive aspects of pain. GMV increase may reflect a remodeling of the central nervous system due to repetitive headache attacks leading to chronic sensitization and a continuous ictal-like state of the brain in chronic migraineurs.

Migrainous Infarction

According to the IHS criteria, migrainous infarction is a typical attack of migrainous aura in a patient with previous history of MA and evidence of cerebral ischemia proven by neuroimaging.

Migrainous infarction is considered a rare complication of migraine. Epidemiologic studies have shown that 0.5–1.5% of all ischemic strokes are migrainous infarctions [33, 34]. Among younger patients with unusual etiology, migrainous infarction was reported to account for 13% of first-ever ischemic strokes [35].

Transient neurologic symptoms are typical for MA, but differentiation among MA, transient ischemic attacks, and migrainous infarction can be very difficult or even impossible on clinical grounds alone. Brain imaging (CT and MRI) is essential for diagnosis of migrainous infarction according to the criteria of the International Headache Society (IHS) [2]. Silent infarctions were detected predominantly in the posterior circulation territory, especially thanks to T2-weighted and FLAIR images [36, 37] (Fig. 4.4). Compared to CT, MRI has proven to be more efficient, especially in acute onsets, since differentiation between migrainous aura and cerebral ischemia can be difficult in the first hours using clinical criteria alone. In these cases DWI provides relevant additional information substantially influencing further management. Given the high sensitivity to detect acute ischemic lesions including even small lacunar or punctuate cortical infarcts, DWI is extremely valuable in the hyperacute phase for positive stroke diagnosis and exclusion of stroke mimics such as migrainous aura symptoms [38–40] and should therefore be preferred in the acute setting.

4.3.1.2 Tension-Type Headache (TTH)

TTH has a high prevalence in general population ranging between 30 and 78% in several studies, and according to ICHD-3 beta [2] and the EHF committee [41], patients with TTH do not exhibit structural brain abnormalities on routine MRI scans. Therefore when clinical features fulfill the diagnostic criteria for TTH, further neuroimaging

investigation is not needed, unless three first-line preventive treatments fail [41]. The pathogenesis of TTH remains incompletely understood. Peripheral pain mechanisms are most likely to predominate in TTH, whereas involvement of central pain mechanisms remains to be determined. Only one study values the functional abnormalities in patients with TTH using fMRI and regional homogeneity (ReHo). Their results suggest that TTH patients exhibit reduced synchronization of neuronal activity in several areas involved in the integration and processing of pain [42]. According to Chen et al. [43], several areas such as primary somatosensory cortex, anterior cingulated cortex, and anterior insula undergo gray matter density dynamic and reversible changes in episodic TTH patients between pain and pain-free phases, valuated with voxel-based morphometry (VBM) analysis.

4.3.1.3 Trigeminal Autonomic Cephalalgias (TACs)

The trigeminal autonomic cephalalgias are a group of primary headache disorders relatively rare in comparison with migraine or TTH. TACs are characterized by pain with a unilateral trigeminal distribution that occurs in association with ipsilateral cranial autonomic features and with typical periodicity or cycling of the attacks and bouts. The group includes cluster headache, paroxysmal hemicrania, hemicrania continua, short-lasting unilateral neuralgiform headache attacks with conjunctival injection and tearing (SUNCT), and short-lasting unilateral neuralgiform headache attacks with cranial autonomic symptoms (SUNA). They differ in attack duration, frequency, and response to therapy. Due to the characteristic presentation, diagnosis is mainly clinical. However the EHF committee recommends for all TACs a brain MRI with detailed study of the pituitary area and cavernous sinus, in order to exclude secondary causes [41, 44]. A recent review reports several structural lesions causing symptoms that are indistinguishable from those of idiopathic TACs: tumors, mainly pituitary adenomas, carotid dissection, cerebral infarctions, trigeminal nerve compression by vascular structures, and multiple sclerosis plaques [45].

In recent times neuroimaging has made substantial contributions to understanding of this syndrome [46]. Iacovelli et al. reviewed several studies which used PET, SPECT, fMRI, MRS, and VBM to better understand the pathophysiology of TACs [47]. All the abnormalities shown by these imaging techniques can be summarized in three major observations: posterior hypothalamic activation during the attacks, involvement of the pain matrix, and involvement of the central opioid system. DTI study results on functional connectivity anomalies in TACs, especially cluster headache, are very diverse and partly contradictory on superficial examination, showing very widespread alterations all over the brain, underlining a complex pain network rather than a single defected structure [48].

4.3.2 Secondary Headaches

Here are several types of headache due to other primary causes and could be classified as follows, according to ICHD-3b secondary headaches (Table 4.1).

The choice of the neuroimaging modality depends on the characteristics of headache: patients with sudden onset and peak intensity of headache should perform an emergent CT

Table 4.1 Causes of secondary headaches according to ICHD-3b

1. Headache attributed to trauma or injury to the head and/or neck
2. Headache attributed to cranial or cervical vascular disorder
3. Headache attributed to nonvascular intracranial disorder
4. Headache attributed to a substance or its withdrawal
5. Headache attributed to infection
6. Headache attributed to disorder of homoeostasis
7. Headache or facial pain attributed to disorder of the cranium, neck, eyes, ears, nose, sinuses, teeth, mouth, or other facial or cervical structure
8. Painful cranial neuropathies and other facial pains

without contrast to rule out intracranial hemorrhage. Additional imaging may be needed depending on the cause of headache at initial findings of CT. Brain MRI is better compared to CT to evaluate the posterior fossa, acute infarcts, and mass lesions. Contrast enhancement should be administrated in suspicion of meningitis, neoplasm, demyelination, and low CSF pressure conditions [49].

4.3.2.1 Headache Attributed to Trauma or Injury to the Head and/or Neck

It is among the most common secondary headache disorders. When a headache occurs for the first time in close temporal relation to trauma or injury to the head and/or neck, it is coded as a secondary headache attributed to the trauma or injury. It has to develop within 7 days of trauma or injury or within 7 days after regaining consciousness and/or the ability to sense and report pain when these have been lost following trauma or injury. Although this 7-day interval is somewhat arbitrary, and although some experts argue that headache may develop after a longer interval in a minority of patients, there is not enough evidence at this time to change this requirement. During the first 3 months from onset, they are considered acute; if they continue beyond that period, they are designated as persistent [2].

Neuroimaging is indicated if there is skull fracture, focal neurologic deficit, or progression of symptoms (Fig. 4.5). With acute head trauma, noncontrast head CT is the primary imaging procedure of choice. MRI with GRE, FLAIR, and SVI and imaging with diffusion-weighted sequence are reserved for severe acute head trauma and in cases in which the patient is much worse on clinical examination than can be explained by CT results. MRI is the primary imaging modality for evaluating delayed effects of brain injury. Furthermore, if MRI and CT are negative but neuropsychological evaluation identifies impairment of mood, executive function, or cognitive endurance, then diffusion tensor imaging might be useful to support the clinical diagnosis [1].

Fig. 4.5 Subdural hematoma; history of trauma in patient with mild left hemiparesis and headache. Axial CT scan: right subdural hematoma with mass effect and median line shift

4.3.2.2 Headache Attributed to Cranial or Cervical Vascular Disorder

Ischemic Stroke

In patients with cerebrovascular event symptoms such as paresis, ataxia and loss of speech are the predominant clinical features. Nonetheless headache has been frequently reported in several studies, with a range of 8–34% [50]. Stroke-related headache can be a sentinel headache (before stroke onset), an onset headache, or a late-onset headache [51], and the characteristic is more similar to the criteria of tension-type headache than migraine [52]. In a lesion mapping study, Seifert et al. found that ischemic strokes that involve the insular cortex, in particular the anterior part, are highly associated with the development of headache. Similar to the insula, the somatosensory cortex has also been demonstrated to be also involved in pain processing during ischemic stroke [50]. Moreover, Chen et al. reported that strokes that arise in the cerebellum, medulla, or

posterior cerebral artery cortex are more likely to be associated with onset headache compared with other cerebral territories [51]. Recently, Seifert et al. found a correlation between headache phenotype and specific lesion patterns: pulsating headache occurred with widespread cortical and subcortical strokes, while tension-type headache was not related to specific lesion pattern [53].

Subarachnoid Hemorrhage (SAH)

SAH is the most common cause of persistent, intense, and incapacitating headache of abrupt onset (thunderclap headache) with a high mortality rate (nearly 50%) and a high disability rate (about 50%) [2]. SAH may be caused by aneurysmal rupture or non-aneurysmal causes [54]:

- Arteriovenous malformation
- Dural arteriovenous fistula
- Cavernous angioma
- Vertebral dissection
- Vasculitis
- Amyloid angiopathy
- Cerebral venous thrombosis
- Reversible cerebral vasoconstriction syndrome
- Perimesencephalic SAH

Unenhanced CT performed within 6 h of symptom onset has 100% sensitivity in detecting SAH as hyperdensity within the subarachnoid spaces. Within 24 h, sensitivity is approximately 93%, falling to 50% at 4 days, with the majority of examinations normal at 10 days, as the aging hemorrhage becomes more isodense to water over time, making it harder to detect in the subacute and chronic phases [54]. A minor bleed may be missed on the initial CT so, if the clinical suspicion remains high, a LP revealing high opening pressure and elevated RBC count should be performed [55]. Although CT remains the exam of choice in the acute setting, MRI can be very sensitive for detection of SAH: T2* sequences have shown sensitivity of 94% in the acute phase (within 4 days) and 100% in the subacute phase (after 4 days), while FLAIR sequences have sensitivity of 81% acutely and 87% in the subacute phase. On T2* sequences SAH is seen as low signal intensity while on FLAIR sequences is seen as hyperintensity in the subarachnoid spaces; however, it should be kept in mind that there are other multiple causes of subarachnoid hyperintensity [49, 54].

After detecting SAH, other imaging investigation should be undertaken to determine the etiology: a ruptured aneurysm account for 80% of non-traumatic SAH. DSA remains the gold standard for the detection of aneurysms, but in the emergency setting, CTA is performed: CTA has 100% sensitivity and specificity for the detection of aneurysms >3 mm; it might be less sensitive and accurate than DSA for aneurysms <3 mm [55]. MRA is a possible alternative to CTA or DSA for aneurysm detection: 3D TOF MRA at high magnetic field (3.0 T) can safely replace DSA in the diagnostic work-up of patients with small aneurysm with a sensitivity of more than 95% [56]. Sacciform aneurysms usually develop at vessel bifurcation or branching points, and most of them occur at typical locations within or near the circle of Willis: the most common locations are the middle cerebral artery bifurcation and along the anterior communicating artery, followed by the origin of posterior communicating artery and ophthalmic artery, while in the posterior circulation, the tip of the basilar artery and the origins of the posterior inferior cerebellar arteries are the most common locations [54]. Hemorrhage localized to the basal cisterns are indicators of aneurysmal SAH, and patterns of hemorrhage help to predict site of aneurysm, particularly ruptured middle cerebral artery or anterior communicating artery aneurysms; parenchymal hematoma is an excellent predictor of the site of a ruptured aneurysm [54]. If the initial angiogram is negative, a second DSA should be performed in the first 2 weeks. The indications for a second DSA include heavy blood load, small aneurysm size, and vasospasm, hematoma, or thrombosis within the aneurysm [49]. In case of negative imaging, in particular DSA, “sine causa” SAH should be considered (Fig. 4.6).

Other Intracranial Hemorrhages

While subdural and epidural hematomas are often related to head trauma, intraparenchymal cerebral hemorrhage (ICH) may underlie several different pathologies (Table 4.2).

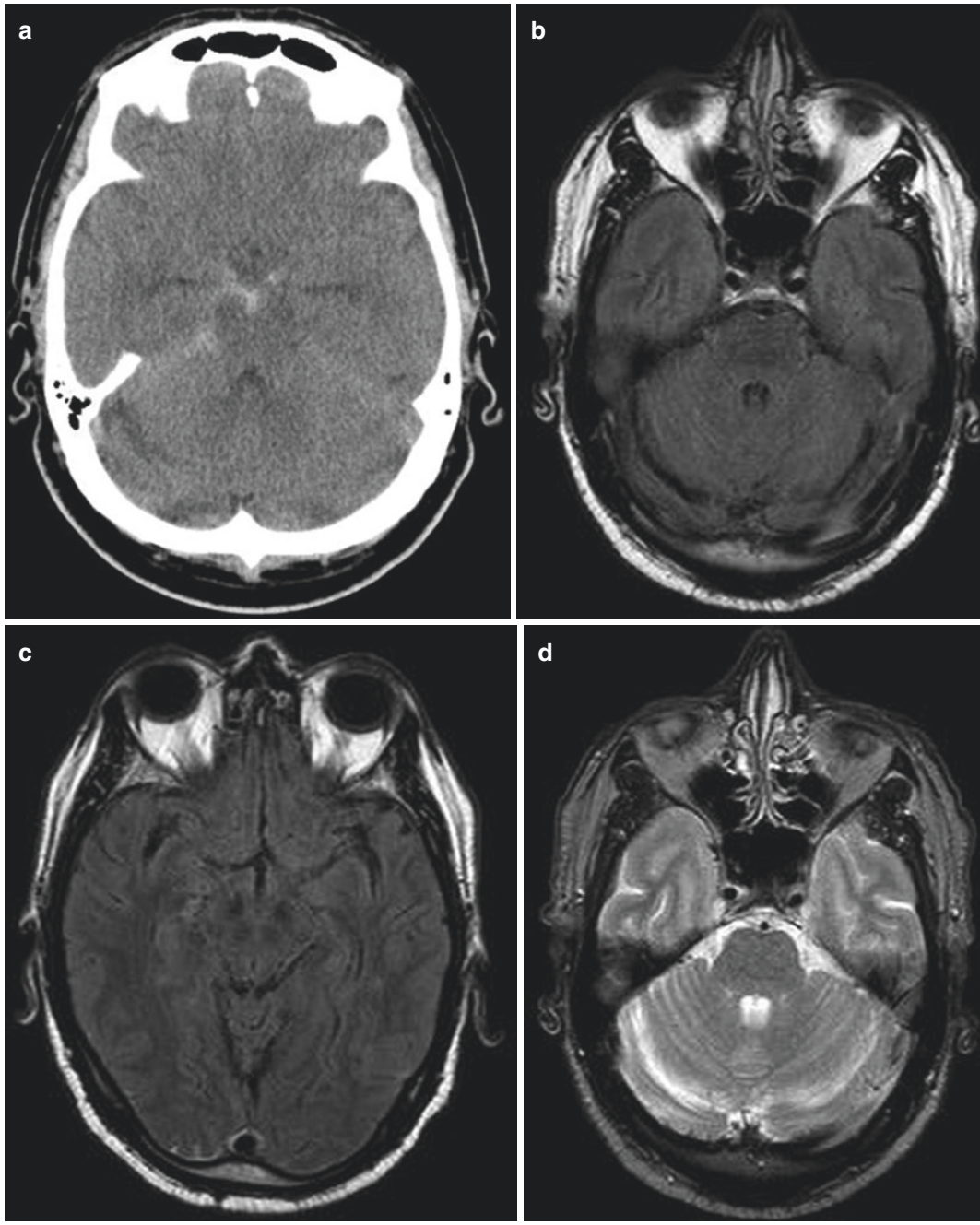

Fig. 4.6 SAH: Patient with thunderclap headache. Axial CT scan (**a**) detects SAH as hyperdensity within the perimesencephalic cistern. On axial FLAIR images (**b**, **c**) mild hyperintense signal is detected in prepontine cistern and temporo-occipital sulci. On T2W image (**d**) only slight linear hypointensity is shown in prepontine cistern

ICH due to hypertension typically affects patients of 60–70 years old and has a 30–50% mortality rate. On CT exam acute ICH due to hypertension classically presents as an intra-axial hyperdense region of hemorrhage centered within the basal ganglia, cerebellum, or occipital lobes. The hemorrhage may vary in size from a relatively small hematoma without significant mass effect to very large hematomas with significant local mass effect and brain herniation that need

emergent surgical decompression or evacuation [57]. Acute ICH in nonclassical intra-axial location or acute ICH in patient younger than 50 should prompt consideration of other causes of bleeding, and additional diagnostic information may be obtained by CTA and/or MRI [57].

Table 4.2 Causes of solitary or multiple intraparenchymal cerebral hemorrhage (ICH)

Solitary ICH	Multiple ICHs
Hypertension	Cavernous malformation
Cerebral amyloid angiopathy	Chronic hypertension
Primary and secondary neoplasms	Cerebral amyloid angiopathy
Cerebral aneurysms	Hemorrhagic metastases
Cerebral arteriovenous malformations	Coagulopathy
Dural arteriovenous fistulae	Cerebral venous thrombosis
Cerebral venous thrombosis	
Coagulopathy	

In cerebral amyloid angiopathy (CAA), the deposition of amyloid-b peptide within cerebral arterial walls results in cerebral microhemorrhages, sulcal SAH, or larger ICH. There are several imaging characteristics to differentiate ICH due to CAA rather than hypertension: ICH secondary to CAA is firstly identified by CT as a hyperdense intra-axial hemorrhage in the subcortical region sparing the basal ganglia, posterior fossa, and brain stem. There may be diffuse white matter hypoattenuation in both cerebral hemispheres that represents underlying microangiopathic changes. MRI may more strongly suggest the diagnosis of CAA by the presence of numerous small microhemorrhages presenting as foci of susceptibility blooming on GRE or SWI sequences in the subcortical white matter sparing basal ganglia, cerebellum, and brain stem. Other typical MRI findings are ICHs at different ages and hyperintensity focal or confluent white matter areas on T2/FLAIR sequences representing microangiopathy [57] (Fig. 4.7).

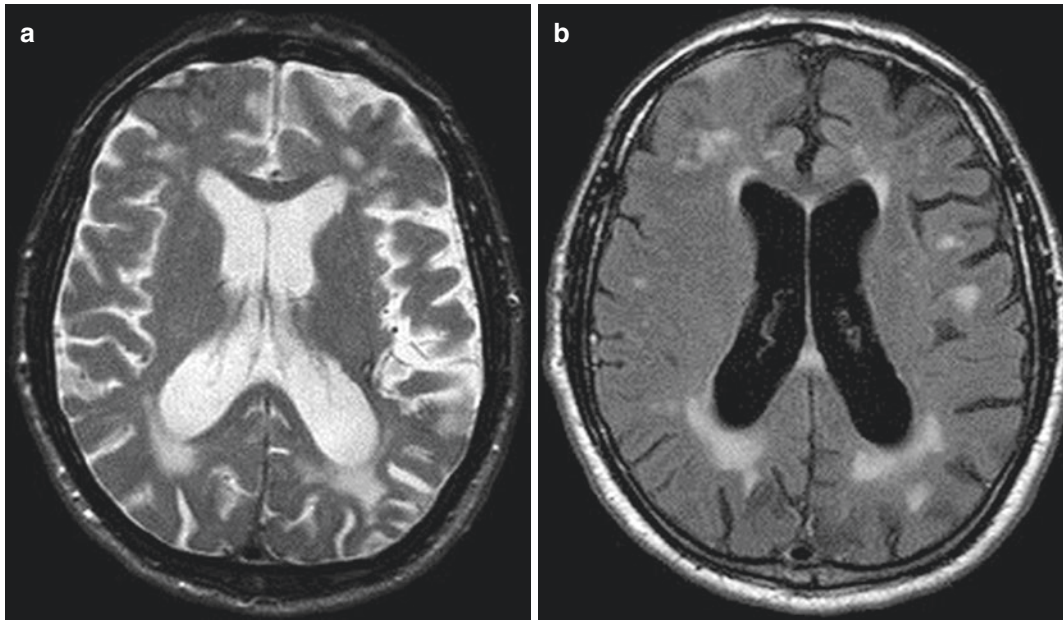

Fig. 4.7 Amyloid angiopathy. Axial SE T2-weighted (**a**) and FLAIR (**b**) sequences show a diffuse enlargement of perimesencephalic subarachnoid spaces associated with focal and partially confluent hyperintense white matter subcortical and periventricular areas. GRE T2* sequence (**c**) allows the identification of cortical, subcortical, and subarachnoid hemosiderin deposition

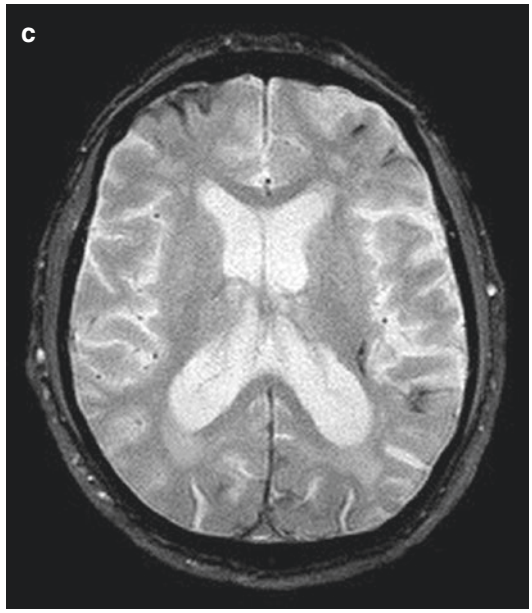

Fig. 4.7 (continued)

Another frequent cause of ICH is cerebrovascular disease which includes aneurysms, arteriovenous malformations (AVMs) (Fig. 4.8), cavernous malformation (Fig. 4.9), dural arteriovenous fistulae (DAVF), hemorrhagic conversion of ischemic stroke, vasculitis, and cortical venous or venous sinus thrombosis.

AVMs are ten times less common than aneurysms and generally affect young patients. They tend to be solitary, and they are composed of a nidus of vessels through which arteriovenous shunting occurs. Their rupture can result with either acute ICH, SAH, or intraventricular hemorrhage (IVH) presenting in the acute setting on CT as hyperdensity within these compartments. AVMs may be identified by CTA, MRA, or DSA. DSA is the gold standard showing a tightly packed mass of enlarged feeding arteries that supply a central nidus; one or more dilated veins drain the nidus, and the abnormal opacification of

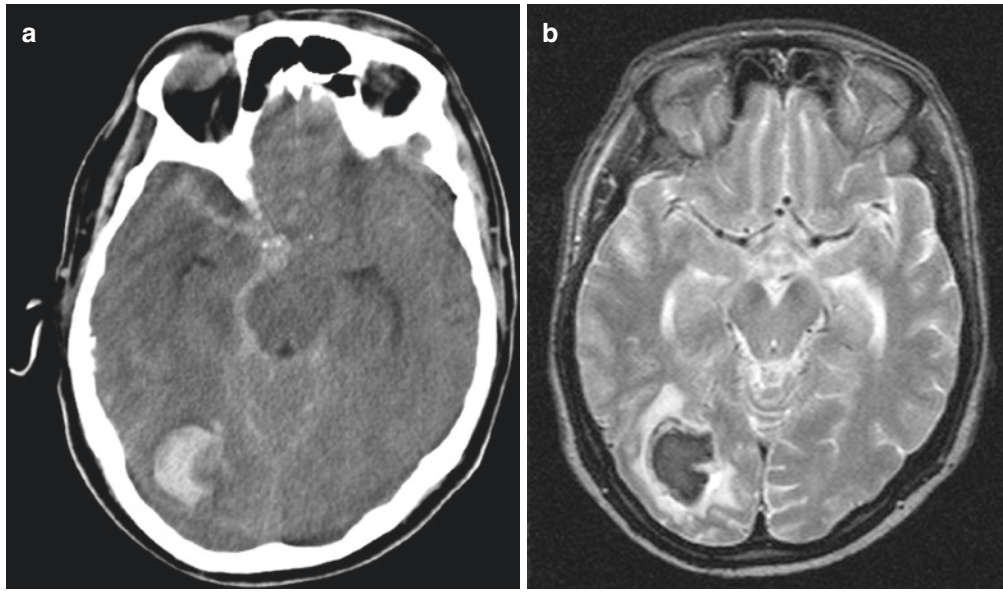

Fig. 4.8 ICH caused by ruptured AVM. On axial CT scan (**a**) a right temporo-occipital ICH, associated with subarachnoid and perimesencephalic hemorrhage, was found. Axial SE T2w (**b**), coronal SE T2w (**c**), and axial SE T1w (**d**) sequences show the early subacute ICH with small vessels along transverse sinus. MRA (**e**) and further DSA (**f**) demonstrate the presence of an underlying AVM associated with dural fistula

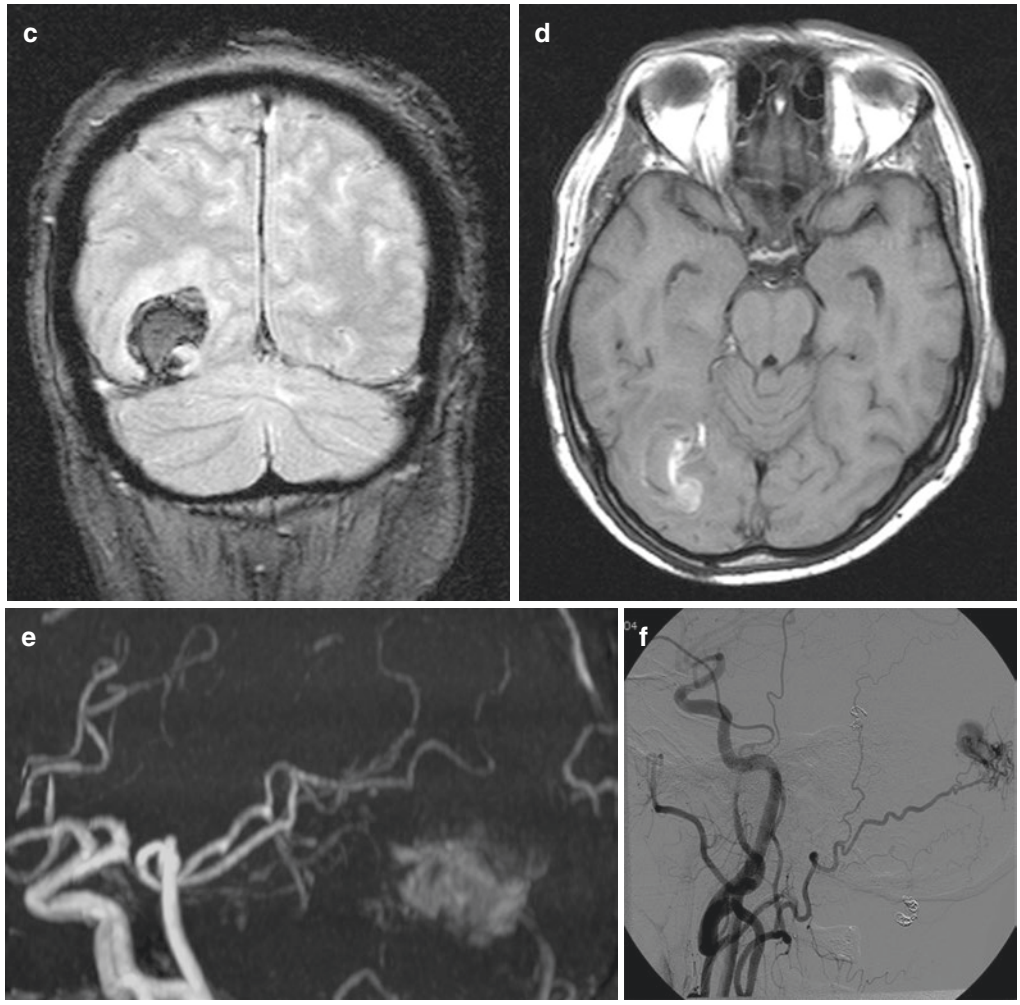

Fig. 4.8 (continued)

veins occurs in the arterial phase, representing shunting. DSA should be performed in every patient presenting with a ruptured cerebral AVM to determine whether the presence of a nidal or perinidal aneurysm may require emergent endovascular or surgical treatment [57, 58].

Headache commonly represents a consequence of ICH or seizures which are the two main manifestations of cavernous malformations [2] (Fig. 4.9): on CT these lesions can be seen as a focal hyperdensity. MRI is the modality of choice demonstrating a typical popcorn appearance with a rim of signal loss due to hemosiderin; the T1 and T2 signal intensity depends on the age of the blood products and fluid-fluid levels may be evident. GRE or SWI sequences have higher sensitivity in detecting small cavernous malformations than conventional SE sequences. When these lesions bleed, they may increase in size on imaging, showing acute ICH and associated vasogenic edema [58].

Cervical Carotid or Vertebral Artery Dissection

Cranial cervical dissection is one of the most frequent causes of stroke in young patients. Headache with or without neck pain can be the only manifestation of cervical artery dissection (Fig. 4.10). It is the most frequent symptom, usually unilateral, severe, and persistent; it can

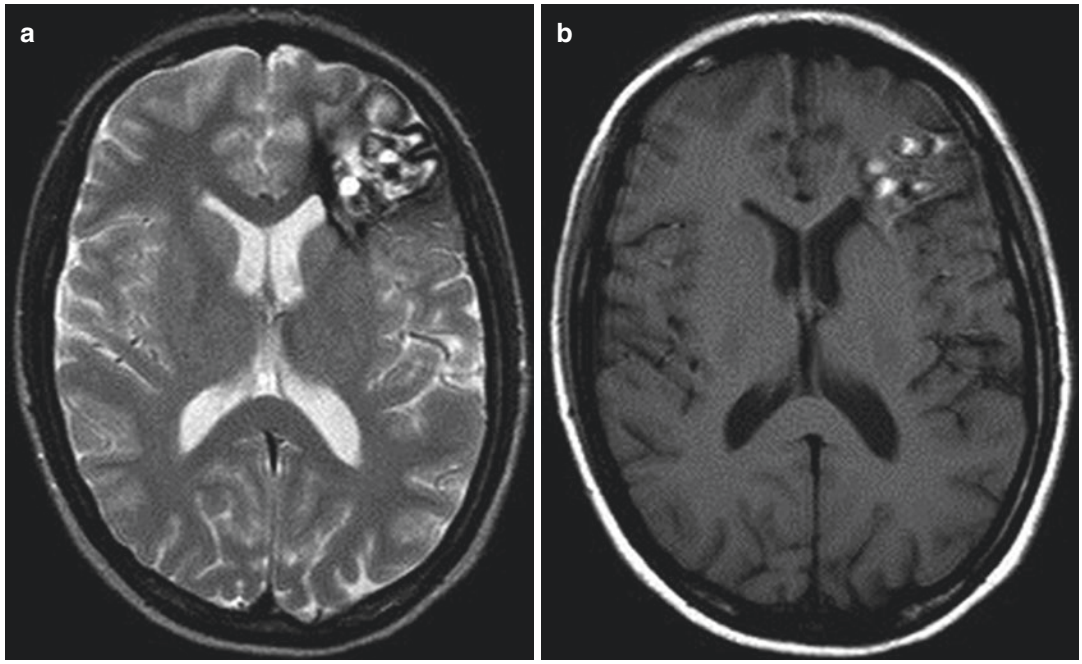

Fig. 4.9 Cavernous malformation in patient with headache. Axial SE T2w (**a**) and SE T1w (**b**) sequences show a large cavernoma in left frontal lobe with subacute bleeding

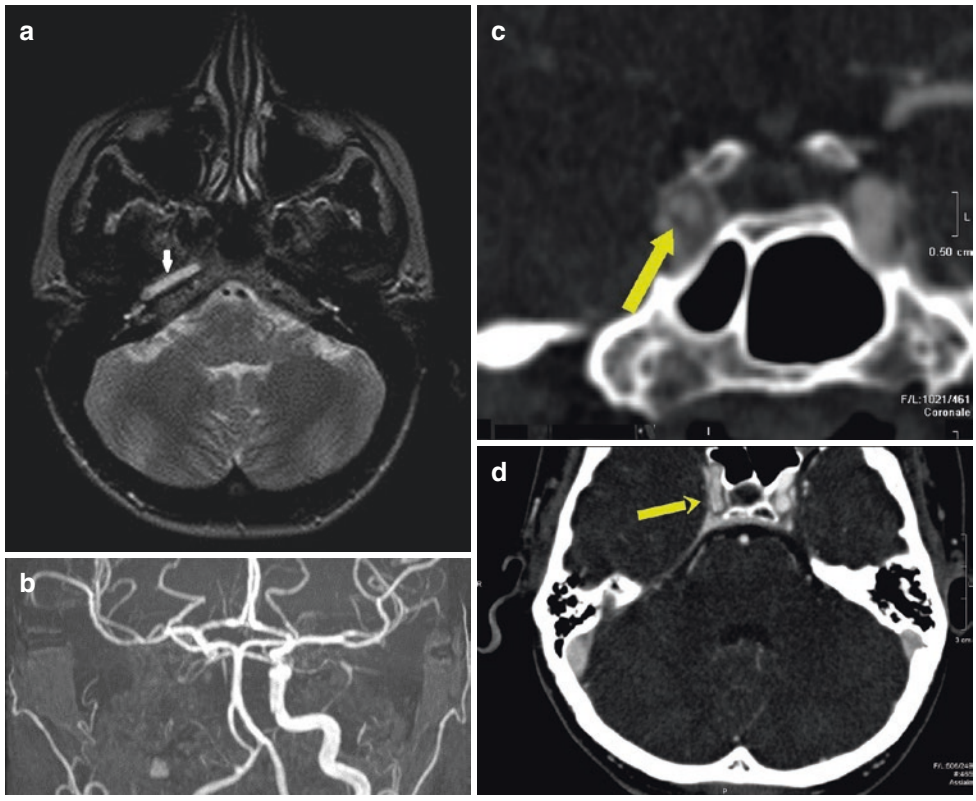

Fig. 4.10 Carotid artery dissection in patient with headache. An hyperintense right carotid artery signal was found on axial SE T2w images (**a**); the lack of visualization of the right carotid artery signal was confirmed on MRA sequences (**b**). A further CTA scan on coronal and axial plane (**c**, **d**) confirmed the presence of a carotid artery dissection flap

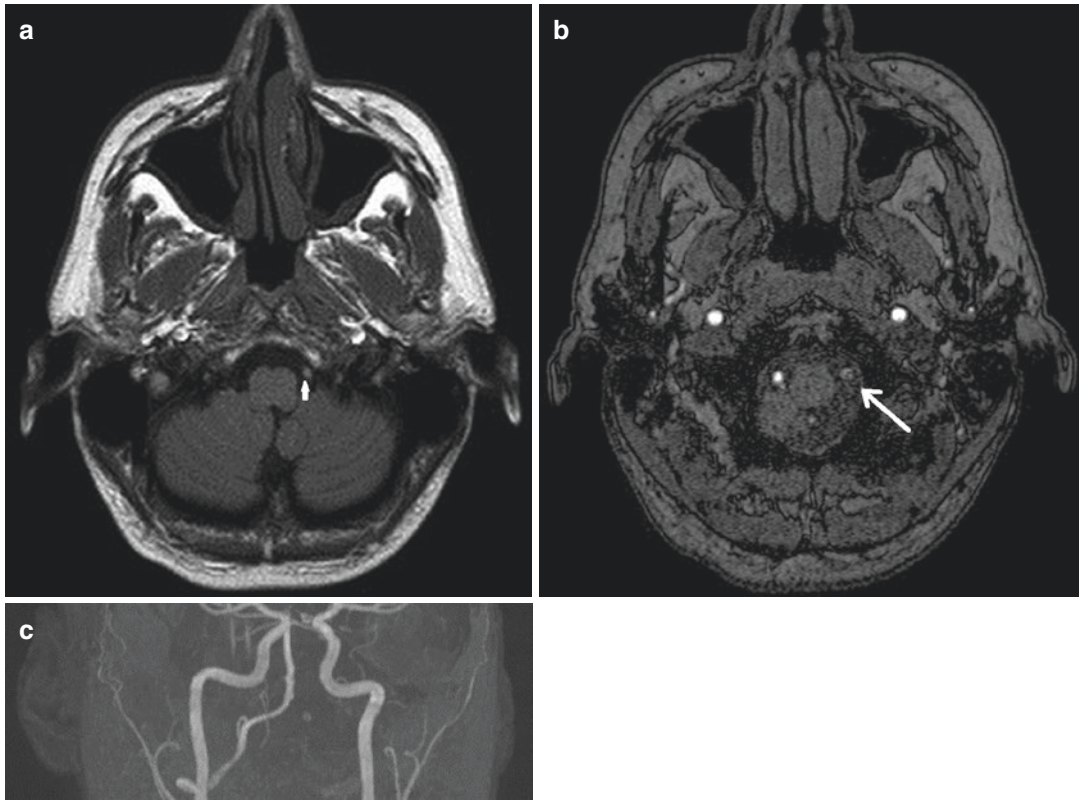

Fig. 4.11 Vertebral artery dissection in patient with acute cervical pain and headache. Axial SE T1w image (**a**) shows a focal hyperintensity in the lumen of the left vertebral artery. MRA source image (**b**) shows the intimal flap within the vessel (arrow), and MIP reconstruction (**c**) confirms the absence of flow signal in the left vertebral artery

remain isolated or precede signs of cerebral or retinal ischemic stroke. Cervical artery dissection may be associated with intracranial artery dissection, which is a potential cause of SAH [2]. The first diagnostic imaging modalities include CTA and MRA. Reported sensitivity and specificity of CTA and MRA for diagnosis of craniocervical arterial dissection are relatively similar, although sensitivity for vertebral arterial dissection may be less [59]; however, a contrast-enhanced MRA may show signal loss within the vertebral artery (Fig. 4.11). Acutely, it is difficult to visualize a dissection on T1-weighted images with fat saturation due to obscuration from the surrounding tissue. In the subacute stage, the dissection appears as a crescent-shaped hyperintensity around an eccentric flow void corresponding to the vessel lumen [49]. DSA is the gold standard, and the angiographic features include luminal narrowing, vessel irregularity, wall thickening/hematoma, pseudoaneurysm formation, and intimal flap [54].

Cerebral Venous Sinus Thrombosis (CVST)

In 80–90% of cases, CVST presents with headache which can be an isolated symptom and may present as thunderclap or progressive headache. Headache may be associated also with focal signs (neurological deficits or seizures) and/or signs of subacute encephalopathy, intracranial hypertension, or cavernous sinus syndrome [2].

Although cerebral angiography is considered the gold standard for the evaluation of CVST, nowadays, CT is usually the first exam performed [60]. Unenhanced CT is often abnormal in patients with neurological signs: a fresh clot is visible as a hyperdensity in cortical veins or dural venous sinuses. This should be confirmed by

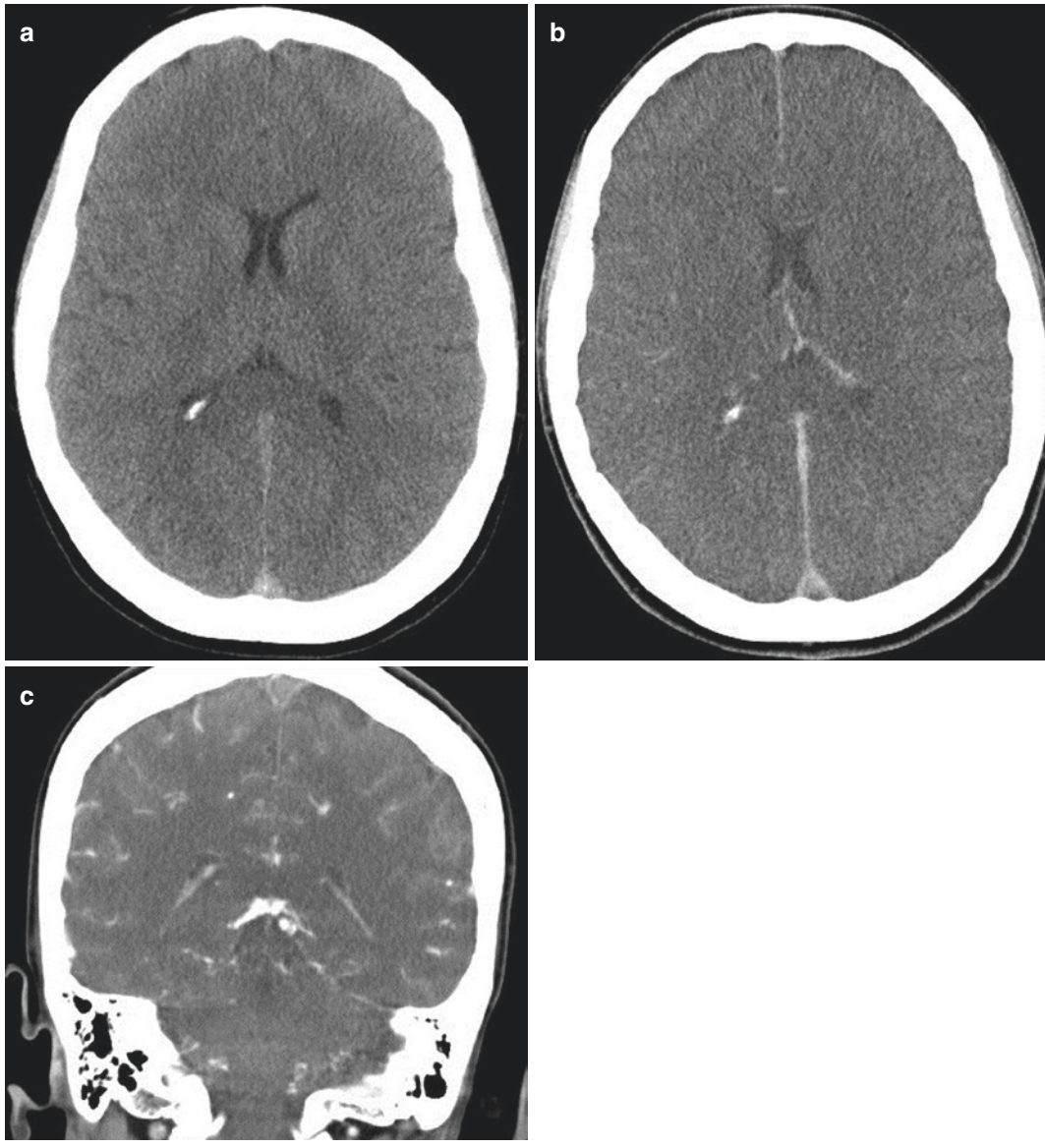

Fig. 4.12 Cerebral venous thrombosis in intractable headache. Axial unenhanced CT scan (**a**) shows hyperdensity in the lumen of the superior sagittal sinus. Axial and coronal contrast-enhanced CT scans (**b**, **c**) confirm the presence of an empty delta sign, representing lack of contrast media filling in venous fresh clot

contrast-enhanced CT (venography CT) showing the hallmark empty delta sign [54] (Fig. 4.12).

On conventional MRI the absence of a flow void and the presence of altered signal intensity in the sinus are primary findings of sinus thrombosis; slow or turbulent flow may also cause altered sinus signal intensity. The signal intensity on T1- and T2-weighted sequences depends on the age of the thrombus: isointense signal on T1-weighted sequences and hypointense signal on T2-weighted sequences in early acute stages (1–5 days), hyperintensity signal on both T1- and T2-weighted sequences from 5 to 15 days, and isointense signal on T1-weighted sequence and hyperintensity on T2-weighted sequences at later stages [49]. T2* sequences may be an important

diagnostic aid: the presence of paramagnetic blood breakdown products (deoxyhemoglobin and metahemoglobin) produces blooming artifacts in the thrombosed venous segment [54]. PD-weighted sequences could also help in the detection of thrombus which appears as a hyperintense defect (Fig. 4.7). Magnetic resonance venography (MRV) with phase-contrast imaging is helpful for the diagnosis and follow-up of CVST. However, MRV may not detect the thrombus, showing only absence of signal in the occluded vein; sometimes it may be difficult to differentiate it from normal anatomic variants such as sinus hypoplasia, flow asymmetry, or arachnoid granulation [49]. Therefore the use of 3D T1-weighted GRE CE sequences is highly recommended as shown by recent studies that demonstrate its highest sensitivity for CVST detection compared with other MRI sequences [60, 61] (Fig. 4.13). Recently, ASL-PWI has been proposed as a further MRI sequence to help identify CVST presenting a bright sinus signal intensity [62]. Cerebral venous thrombosis results in an increased venous pressure that can lower cerebral perfusion pressure and induces parenchymal changes due to vasogenic edema, cytotoxic edema, intracranial hemorrhage, and subarachnoid hemorrhage [62]. Edema can be predominantly cytotoxic or vasogenic, hence with mixed DWI signal alterations (Fig. 4.8). CVST leads to venous infarction in about 50% of cases, but distribution of venous drainage areas is subject to variation. However, there are some characteristics that may guide to proper diagnosis: bilaterally involvement of deep structures (cerebral deep vein thrombosis) or parasagittal regions (sagittal sinus thrombosis), as well as uni- and bilateral changes in peripheral areas of brain lobes or the temporal lobe (cortical vein thrombosis) [54]. Parenchymal hemorrhage is present in 30% of cases: flame-shaped, irregular zones of lobar hemorrhage in the parasagittal frontal and parietal lobes are typical findings in patients with superior sagittal sinus thrombosis,

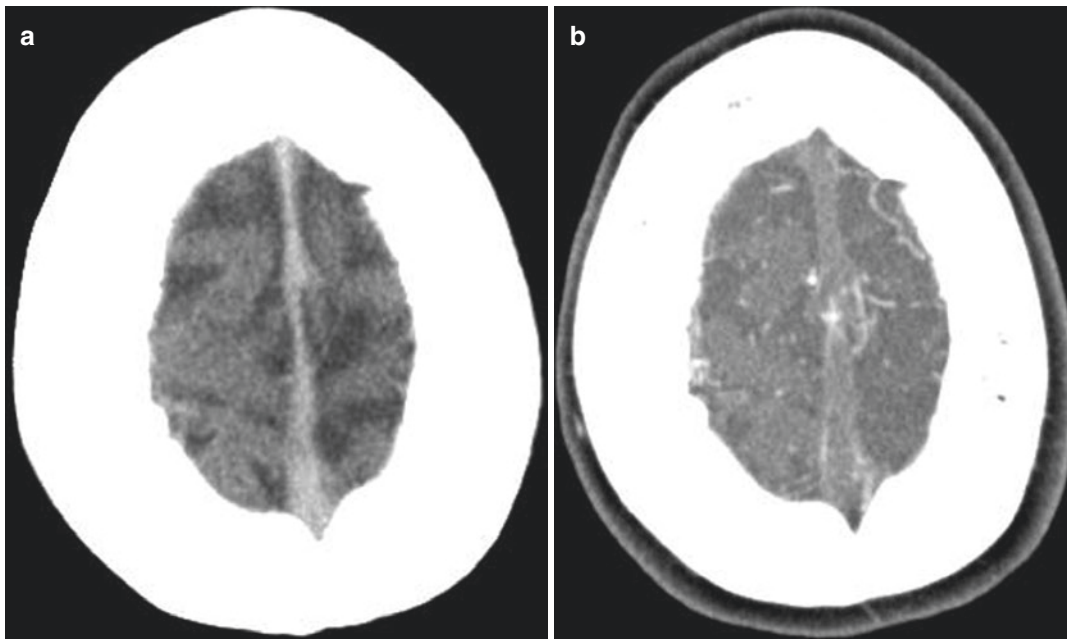

Fig. 4.13 Cerebral venous thrombosis in patient with headache. Unenhanced CT scan (**a**) shows hyperdensity in superior sagittal sinus (SSS) with empty delta sign on enhanced CT (**b**). MRI shows hyperintense signal at the level of frontoparietal sulci on FLAIR image (**c**); it confirmed the presence of a subacute thrombus in SSS and cortical veins on T1 w image (**d**) and lack of opacification after contrast media (**e**, **f**). Follow-up scan demonstrated resolution of the thrombosis with disappearance of hyperintensity on FLAIR image (**g**), thrombus on T1w image (**h**), and complete opacification of SSS (**i**, **j**)

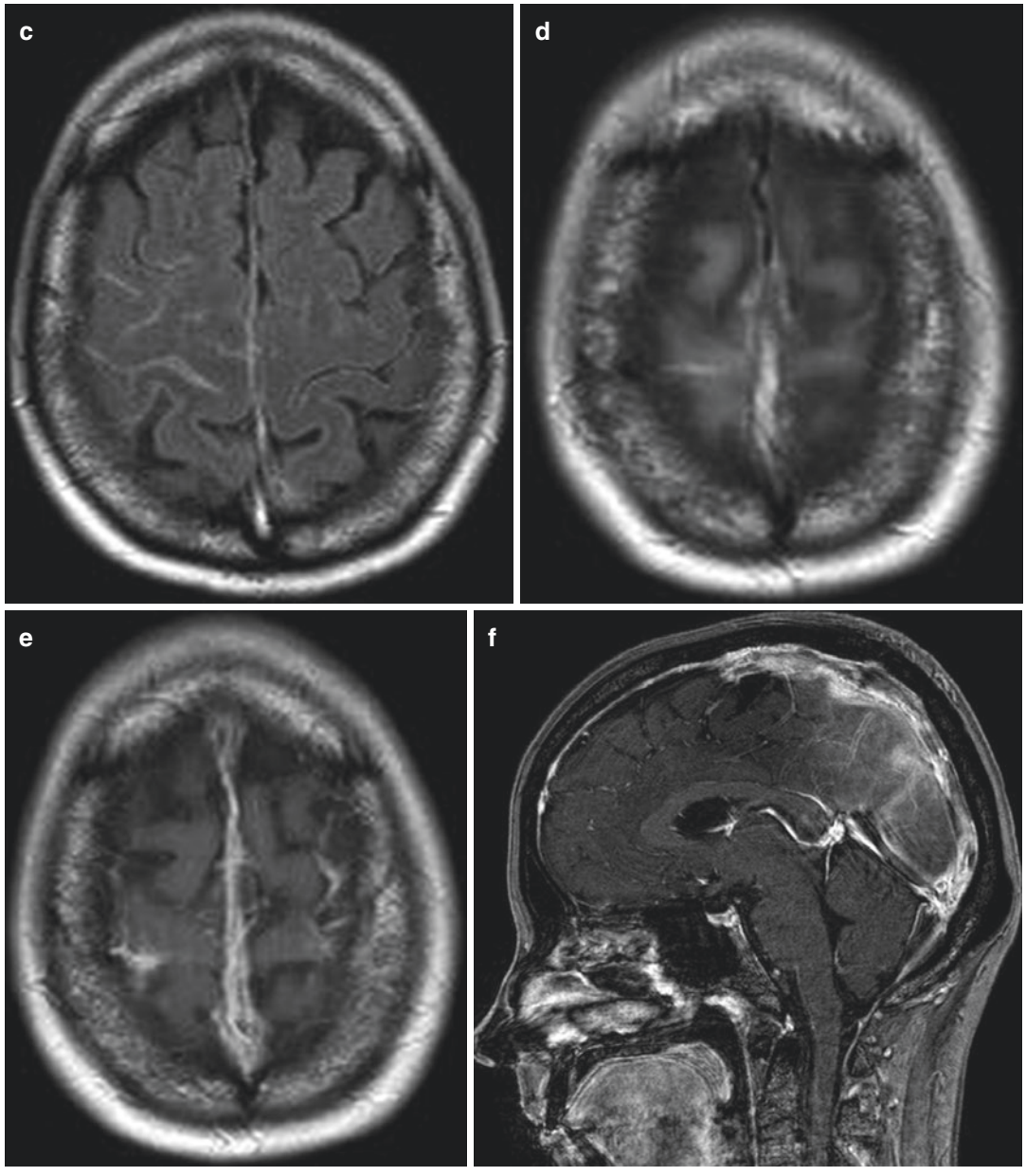

Fig. 4.13 (continued)

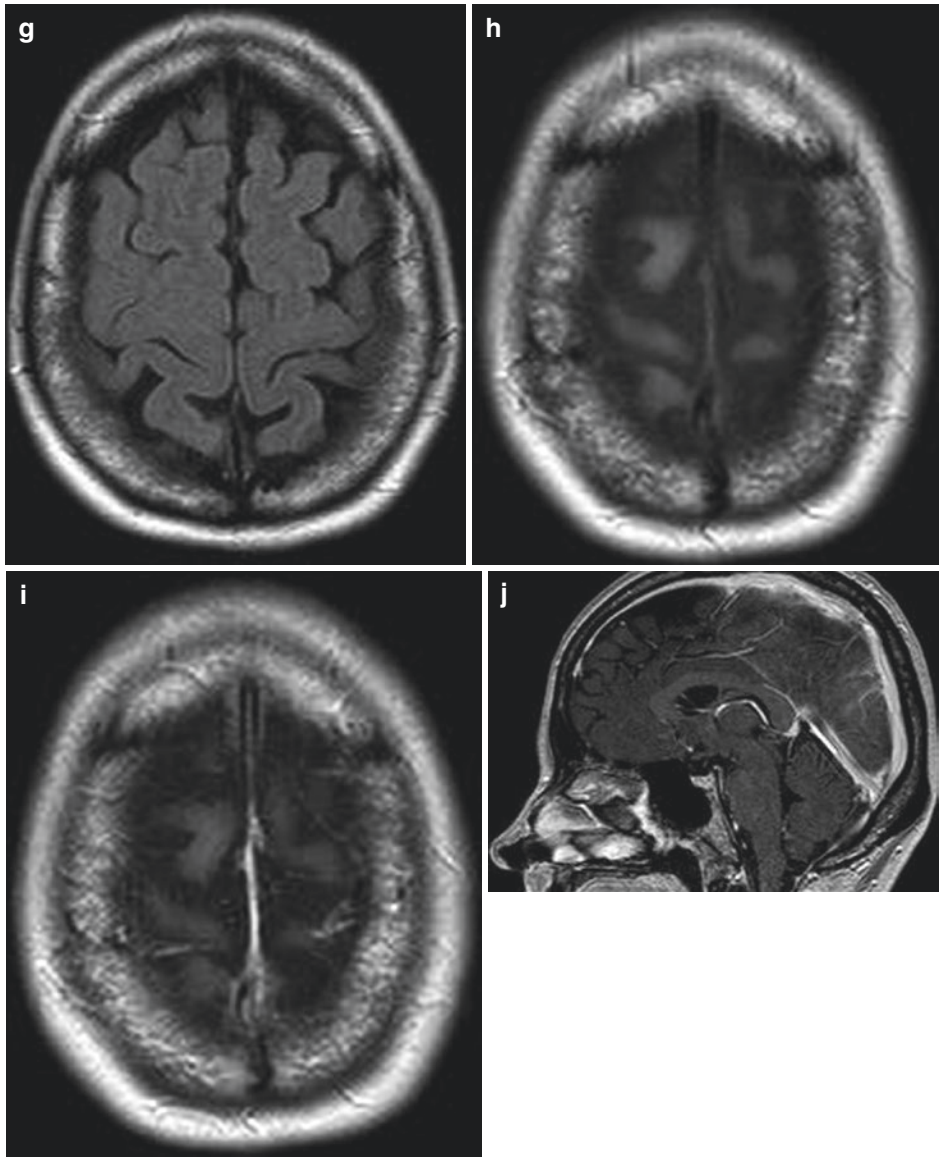

Fig. 4.13 (continued)

whether hemorrhage in the temporal and occipital lobes is more typical of transverse sinus thrombosis. T2* sequences have high sensitivity in the depiction of parenchymal hemorrhage. Rarely CVST may be associated also with SAH [54]. Recent studies evaluated the usefulness of ASL-PWI sequences to determine the hypoperfusion of brain parenchyma drained by the thrombosed sinus, showing a decreased CBF in the affected area [62].

Reversible Vasoconstriction Syndrome (RCVS)

RCVS is a term used to group reversible angiopathies that present with a sudden thunderclap headache with or without focal neurological deficits and/or seizures, recurrent in 1 month and triggered by several factors such as sexual activity, exertion, and Valsalva maneuver. Typically RCVS presents with multifocal arterial vasoconstriction. During the first week after clinical onset, neuroimaging investigation can be normal [2]. Abnormal findings may develop later, revealing cortical SAH over the convexities of the cerebral hemispheres, intracerebral hemorrhage (ICH), infarction in a watershed zone, or brain edema [49]. Ischemic stroke is the most common, followed by isolated convexity SAH and isolated ICH. Brain infarcts and hemorrhages are typically located in watershed zones, usually in posterior regions, in a pattern which can be similar to that of an atypical posterior reversible leukoencephalopathy syndrome (PRES) (there is a 10% overlap with this condition) [54] (Figs. 4.14 and 4.15).

MRI may be more sensitive than CT for detecting subtle cortical SAH, cerebral edema, infarction, and leukoencephalopathy. The gold standard for diagnosis is DSA which detects the typical alternating areas of arterial constriction and dilatation, often called "beading," in multiple vascular beds [63]. These alterations are usually bilateral and multiple and affect all intracerebral arteries and their branches, while the extracranial segments of the internal carotid and vertebral arteries are rarely involved. These changes usually resolve within 3 months [54, 64]. CT angiography and MRA are alternative and less invasive methods for identifying the arterial changes [63]. Furthermore, the ASL MRI perfusion maps may reveal hypoperfusion of several cerebral areas as reported by Komatsu et al. [65].

Cerebral Autosomal Dominant Arteriopathy with Subcortical Infarcts and Leukoencephalopathy (CADASIL)

CADASIL is the most common monogenetic cause of adult onset progressive cerebrovascular disease. It is an autosomal dominant arteriopathy characterized by migraine usually with aura presenting in early adulthood (at a mean age of 30), recurrent ischemic events, mood disturbances, progressive cognitive impairment mostly affecting executive function, and acute encephalopathy [49, 66]. Onset of radiologic manifestations closely mirrors the onset of migraine with mean age of imaging abnormalities starting at 30 years. By the age of 35, essentially all patients with CADASIL have abnormal MRI findings [66]. MRI is the most clinically relevant imaging modality. In early stages nonspecific periventricular and subcortical hyperintensities on T2/FLAIR sequences may be seen. The typical radiologic findings of advanced stages of CADASIL are confluent, large, symmetrical white matter changes on T2/FLAIR sequences, particularly in the anterior temporal poles, external capsula, and superior frontal gyrus [66]. Anterior temporal pole alterations have a high sensitivity and specificity for this disease (approximatively 90% for each) (Fig. 4.16). DWI sequences may show acute and subacute ischemic events. GRE sequences may show in a variable number of cases (30–70%) cerebral micro-bleeds most commonly affecting the thalami, basal ganglia, and brain stem [66, 67]. The MRI findings that are most strongly related to clinical deficit are number and volume of lacunes, brain atrophy, and white matter disease [68]. Recently DTI has been used to characterize tissue damage in CADASIL: DTI helps demonstrating the extensive microstructural changes involving intra- and interhemispheric cerebral, thalamocortical, and cerebro-cerebellar connections; moreover the severity of microstructural changes correlates with extension of T2/FLAIR hyperintensities [69].

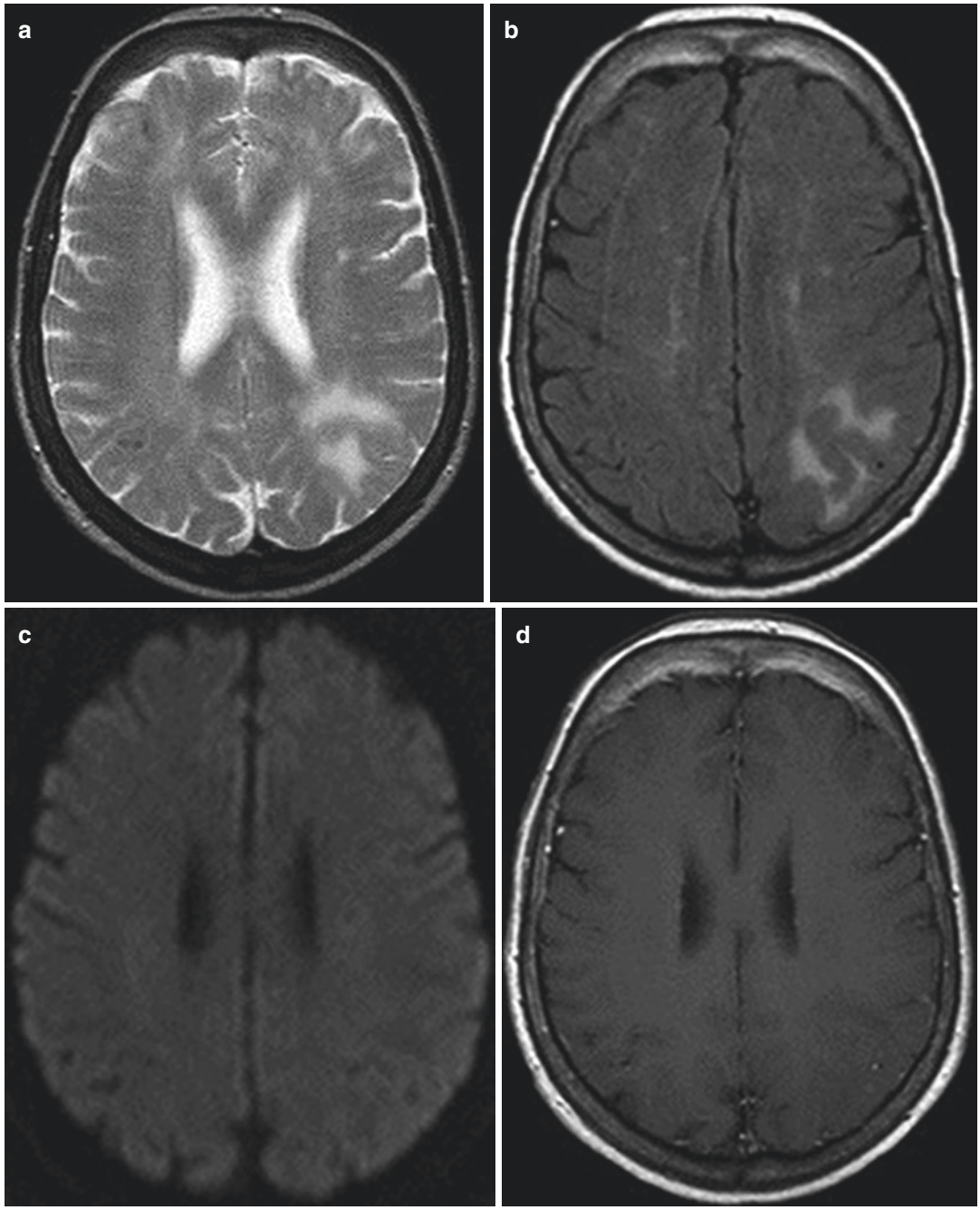

Fig. 4.14 RCVS in patient with thunderclap headache and seizures. Axial SE T2w (**a**) and FLAIR (**b**) sequences show a left parietal subcortical white matter hyperintensity, sparing the cerebral cortex, with no significant alterations on DWI (**c**) and SE T1w + Gd (**d**) sequences. The GRE T2*w sequence helps identify parietal and frontal SAH (**e**)

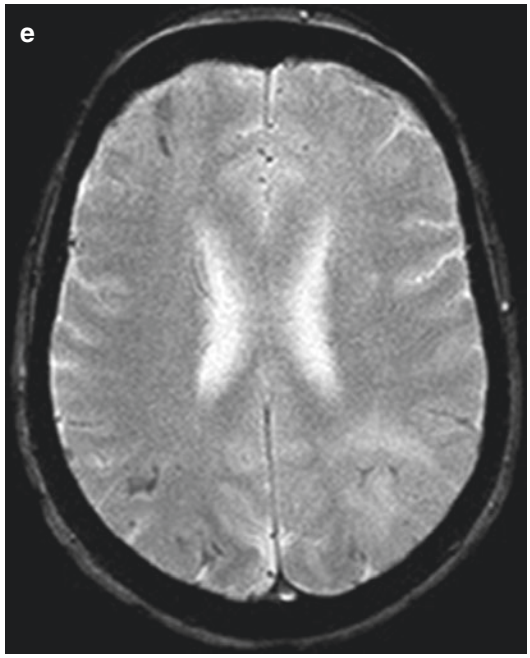

Fig. 4.14 (continued)

4.3.2.3 Headache Attributed to Nonvascular Intracranial Disorders

Spontaneous Intracranial Hypotension

Spontaneous intracranial hypotension (IH) occurs as a result of spinal cerebral fluid leak due to iatrogenic, traumatic, or spontaneous causes. Typically IH presents with orthostatic headaches associated with other symptoms such as neck pain, tinnitus, change in hearing, photophobia, and nausea. Some patients however do not present classical symptoms, but show atypical clinical presentation with non-orthostatic headaches or absence of headaches [70]. CT has little diagnostic value although subdural fluid collections or increased tentorial enhancement may be detected [49]. MRI with gadolinium administration has an important role in diagnosis of IH, particularly in atypical clinical presentation. Typical MRI findings of

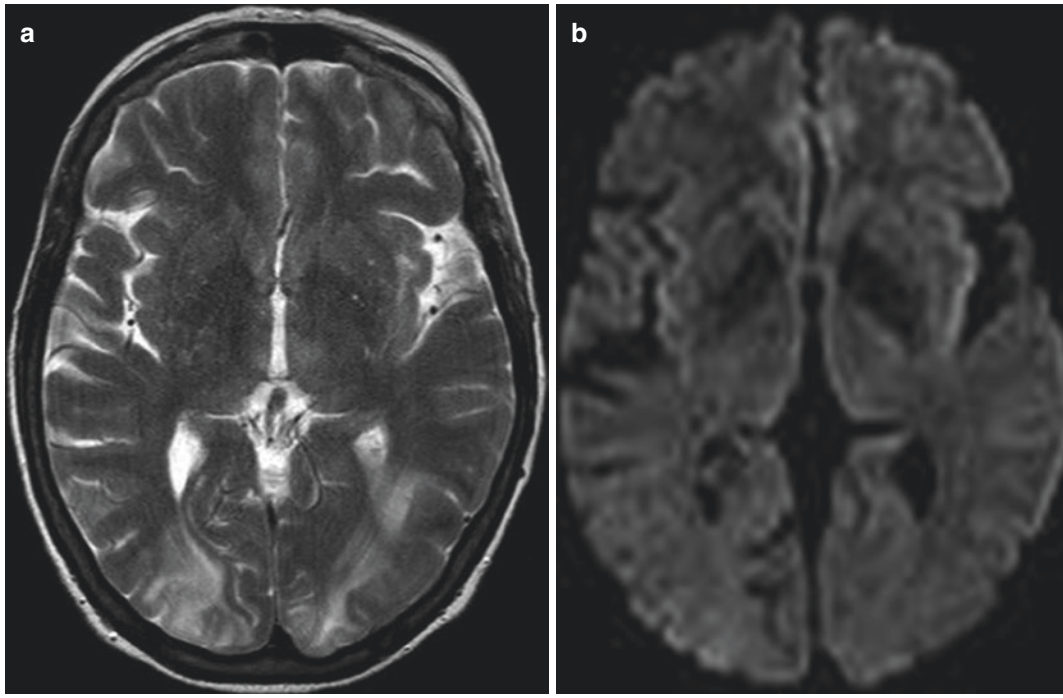

Fig. 4.15 Patient with prolonged severe hypertension and headache—PRESS. Bilateral parieto-occipital cortical-subcortical focal hyperintensities on axial SE T2w images (**a**) with no signal restriction on DWI (**b**). MRI control after 3 weeks (**c**, **d**) shows no focal alterations with complete resolution of the previous findings

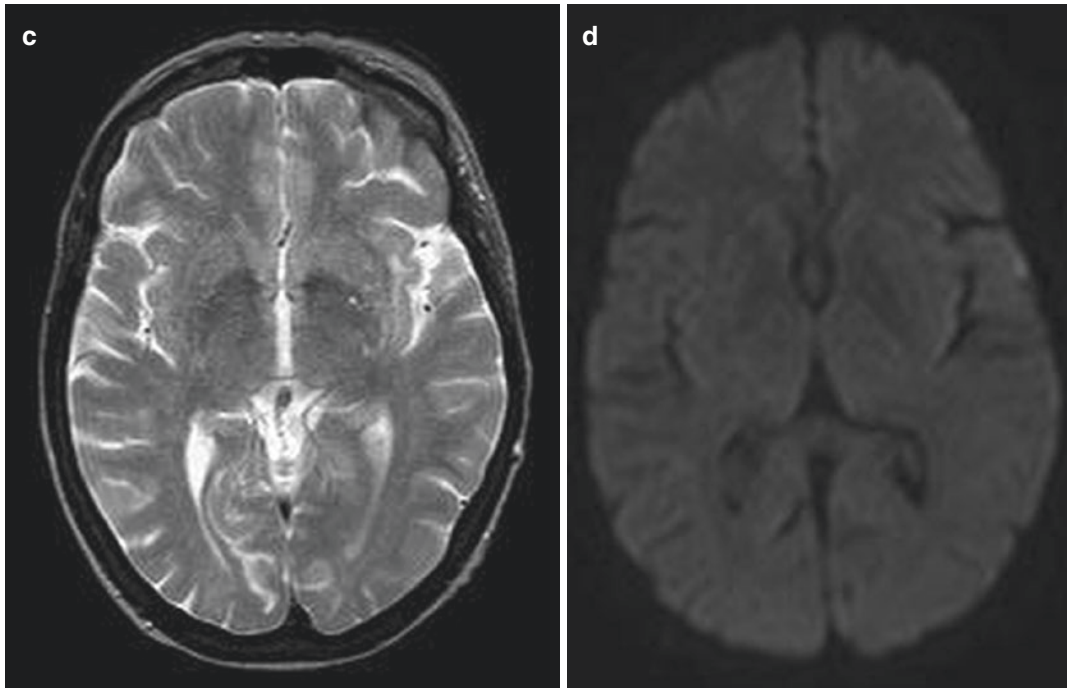

Fig. 4.15 (continued)

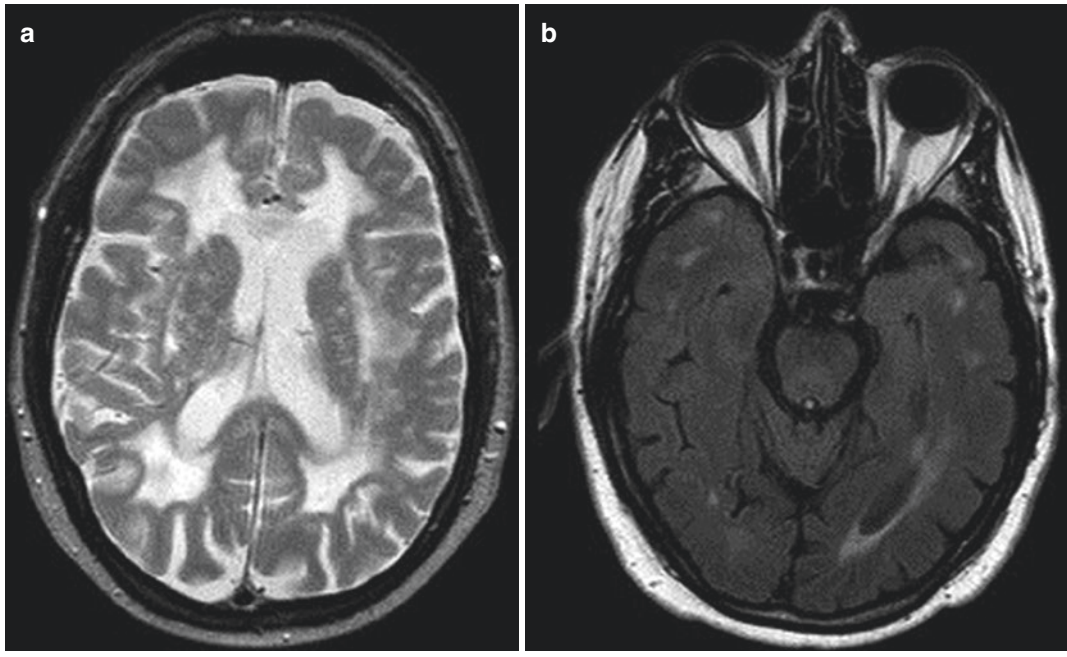

Fig. 4.16 Recurrent headache and stroke episodes in patients with CADASIL. Large, confluent, symmetrical subcortical white matter hyperintensities on SE T2w (**a**) and FLAIR (**b**) sequences, with involvement of the external capsula and the anterior temporal poles

IH include diffuse, non-nodular, pachymeningeal enhancement, engorgement and enhancement of cerebral venous sinuses, and pituitary gland enlargement. Coronal and sagittal images may show downward displacement of the brain, tonsillar herniation, flattening of the pons and optic chiasm, and decreased size of subarachnoid cisterns [49, 70]. Subdural fluid collections may be present as a late finding of untreated IH; when moderate or large in size, there can be secondary hemorrhage causing subdural hematomas because of stretching and rupture of bridging veins [70]. Spine abnormalities associated with IH can be detected with MRI, and they include extra-arachnoid fluid collections, spinal meningeal enhancement, engorgement of epidural venous plexus, and intradural spinal veins [70, 71]. A coronal MR myelography has been recommended for detecting the leakage of CSF as a first-choice modality, followed by axial MRI and if necessary CT myelography [70] (Fig. 4.17).

Increased Cerebrospinal Fluid Pressure

CSF circulatory dysfunction can likewise be a source of headache. A particular form of this is the cerebral pseudotumor, which can arise as a primary disorder (idiopathic intracranial hypertension) or from secondary causes such as exogenous agents or venous sinus thrombosis [49].

The most common diagnostic sign is papilledema on the fundoscopic exam. Visual acuity and visual fields using perimetry need to be documented on these patients because of the potential for visual loss. A lumbar puncture opening pressure of at least 259 mm supports the diagnosis of pseudotumor cerebri syndrome [49].

CT or MRI of the brain is required prior to performing the diagnostic lumbar puncture to rule out a space-occupying lesion. CT should be normal and without evidence of intracranial mass or hydrocephalus.

MRI is the examination of choice to help support the diagnosis. Typical imaging findings are flattening of the papilla in axial T2w images as well

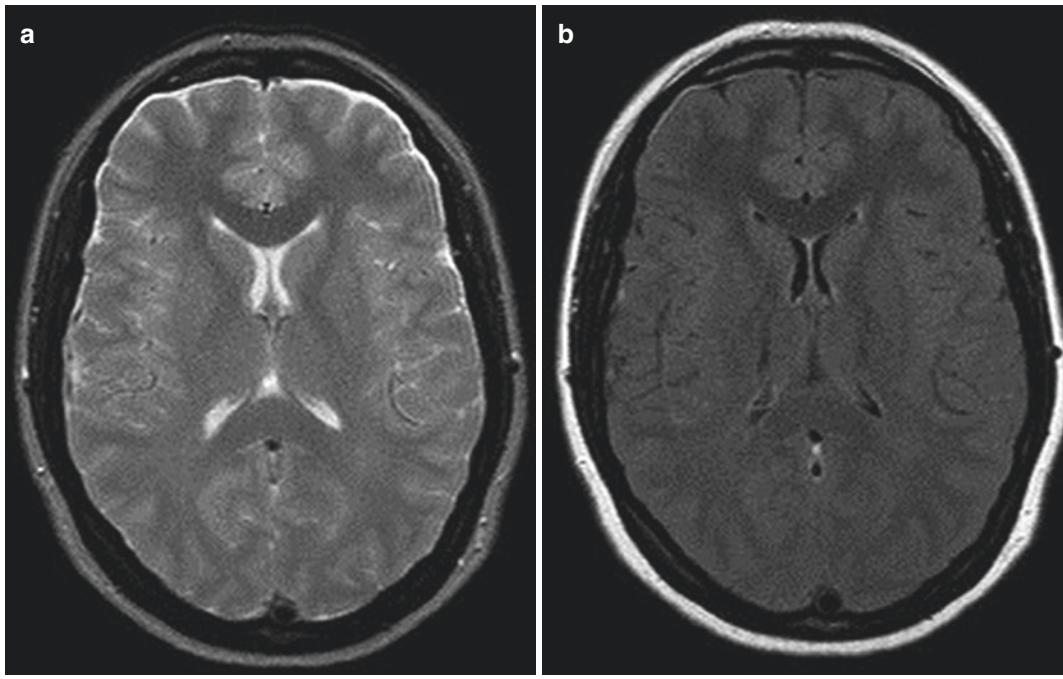

Fig. 4.17 Long-standing intractable headache in patient with spontaneous intracranial hypotension. T2w image (**a**) shows slight enlargement of subdural frontal space. A subtle hyperintense subdural collection is seen on FLAIR image (**b**) and diffuse thickening and pachymeningeal enhancement is seen on T1w image after contrast media (**c**). Myelo-RM (**d**, **e**) well demonstrates spontaneous CSF leakage at the level of C2–C3

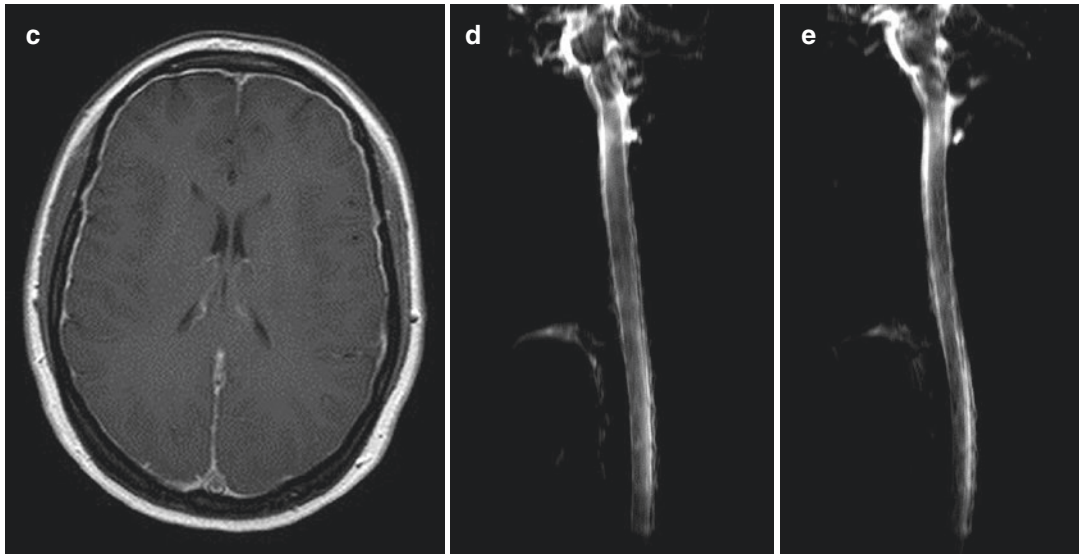

Fig. 4.17 (continued)

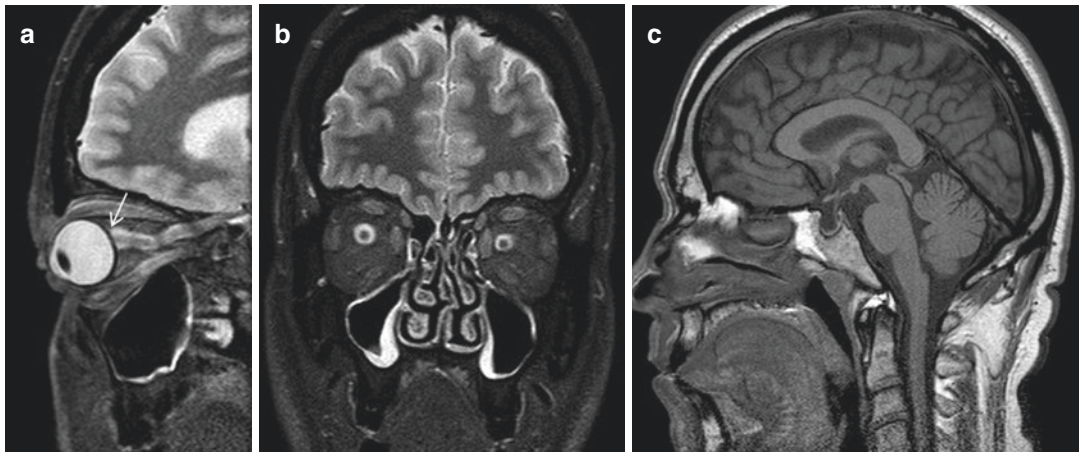

Fig. 4.18 Intracranial hypertension and headache. Sagittal (**a**) and coronal (**b**) STIR images and sagittal SE T1-weighted image (**c**) show flattened posterior sclera (arrow) (**a**), prominent subarachnoid space around the optic nerve (**b**), and partial empty sella (**c**)

as a gyrose optic nerve. Coronal images reveal an enhancement of the optic nerve sheath; this phenomenon can be easily assessed using T2w images with fat saturation. Additionally, sagittal views frequently reveal that the pituitary gland is flattened (so-called empty sella syndrome) or tonsillar descent (Fig. 4.18). Venous angiography frequently reveals stenosis in the transverse sinus [72].

Intracranial Neoplasia

Headaches caused by brain tumors have been classically described as severe, early morning, or nocturnal headaches associated with nausea and vomiting. In these types of patients, headache has developed in temporal relation to the intracranial neoplasia or let to its discovery. It usually significantly worsens in parallel with worsening of the

intracranial neoplasia and may significantly improve in temporal relation to the successful treatment of the neoplasia [2]. However, several studies have shown that headaches arising from brain tumors can present with the same phenotype as primary headache disorders such as migraine or tension-type headaches. Most patients have atypical features, and only 17% of patients fit the classic brain tumor headache descriptions [73].

Imaging, both CT and MRI, rules out space-occupying lesions or hydrocephalus. MRI, however, is more sensible than CT for the detection and evaluation of the extension of the tumor. This is particularly true for some brain regions (such as sellar, auditory canal, etc.) or meningeal pathology (Fig. 4.19). A particular case of tumor, which causes headache, is the *colloid cyst*. This is a protein-rich cyst of the roof of the third ventricle emanating from the endoderm [74]. Colloid cysts can be an incidental finding in cranial imaging or can manifest themselves with headaches. Headaches arising from a colloid cyst of the third ventricle are often thunderclap and recurrent. Headaches

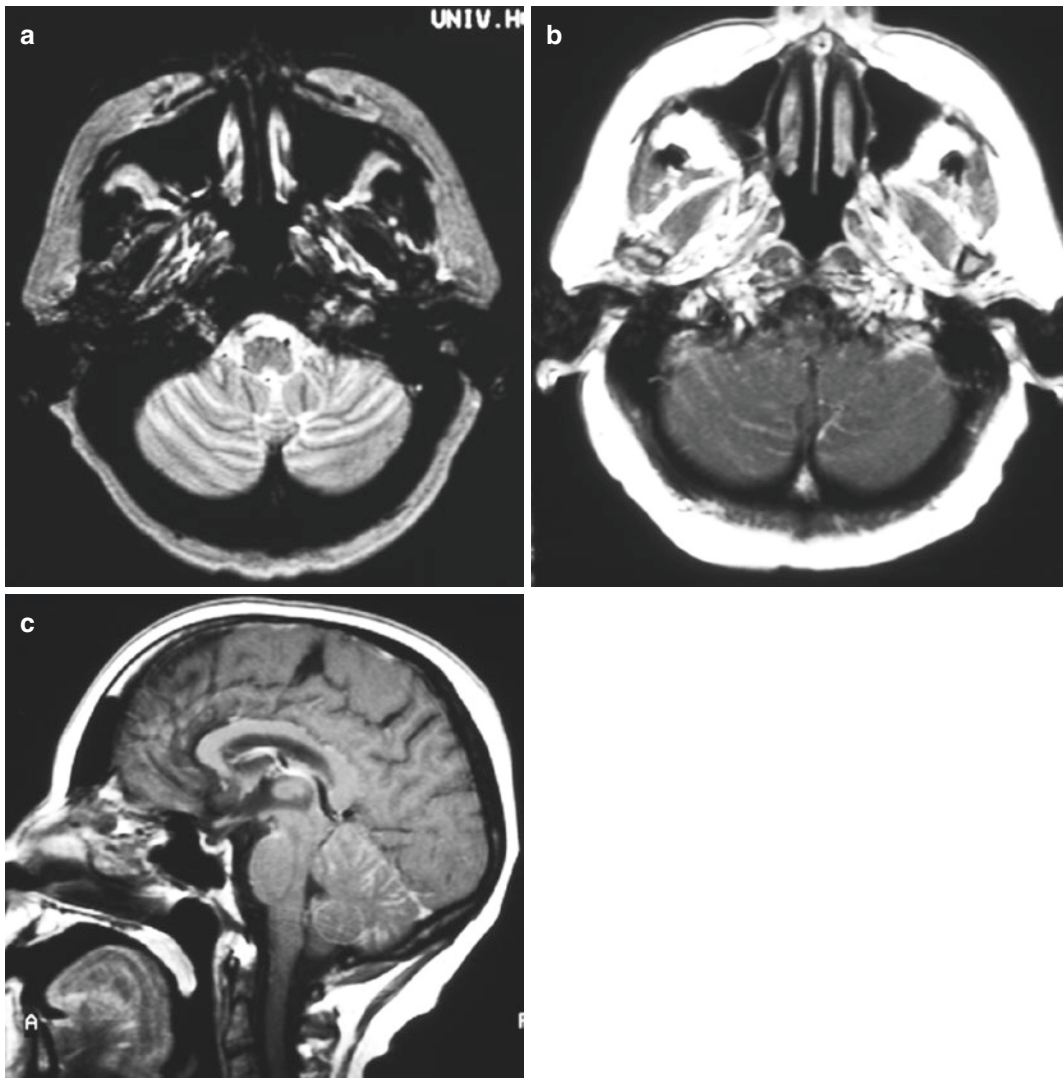

Fig. 4.19 Carcinomatous meningitis—intractable headache in patient with previous breast cancer. Axial SE T2w image (**a**), axial and sagittal SE T1w image after Gd (**b**, **c**): mild enlargement of the cerebellar sulci on T2W images (**a**) and diffuse leptomeningeal enhancement on T1W images after CM (**b**, **c**)

may improve in the supine position and are often located in the bilateral frontoparietal or fronto-occipital regions. The cyst may cause obstructive hydrocephalus as it is located close to the foramen of Monro. There are no restricted diffusion and hyperintensity seen on FLAIR sequences. On T1-weighted images, the central portion of the mass is hyperintense, whereas the periphery is isointense. The central portion is markedly hypointense, while the peripheral portion is isointense in T2-weighted images [75] (Fig. 4.20).

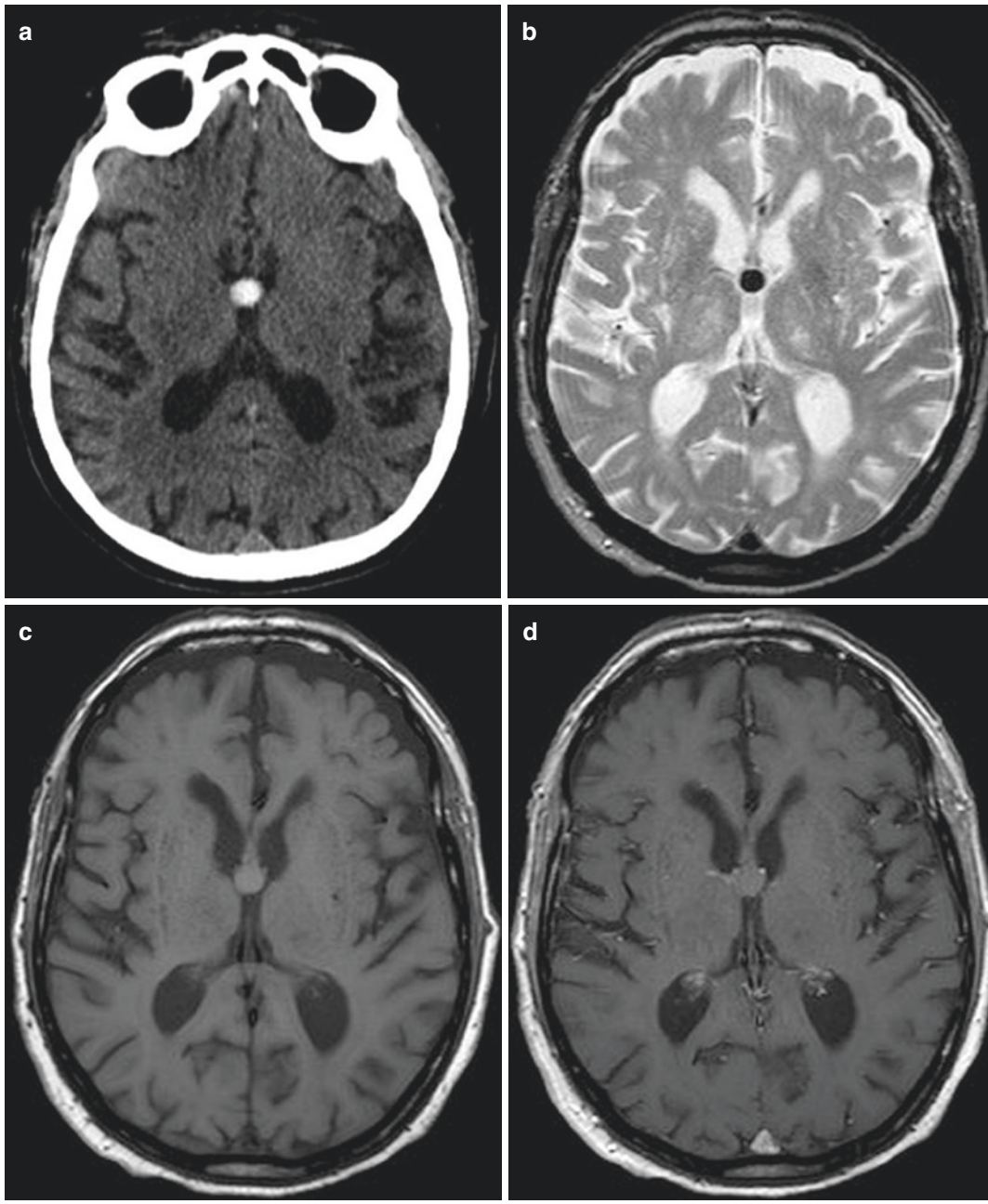

Fig. 4.20 Colloid cyst in patient with positional headache. Hyperdense cyst in the third ventricle at the level of Monro foramen is visible on axial CT scan (**a**). It appears hypointense on axial SE T2w sequence (**b**) and hyperintense on axial SE T1w sequence (**c**) and does not enhance after Gd administration on SE T1 sequences (**d**)

Chiari Malformation Type I

Chiari malformation type I (CM1) headaches are often precipitated by cough or Valsalva maneuver. There may be associated symptoms of brain stem, cerebellar, or cervical dysfunction. The associated headaches are occipital or suboccipital and generally last longer than primary cough headaches which last several seconds to a few minutes (although some patients experience mild to moderate headache for 2 h) [2]. MRI is required for the diagnosis to obtain detailed sagittal images. Brain MRI shows at least 5 mm of caudal descent of the cerebellar tonsils which appear "peglike" and pointed. Other MRI findings include crowding of subarachnoid space at craniocervical junction and kinking of the medullary cervical junction and brain stem [76]. Tonsillar herniation of less than 5 mm does not exclude the diagnosis, if other features on brain MRI are present and patient is symptomatic. Asymptomatic tonsillar ectopia may be differentiated from symptomatic CM1 using CSF flow studies. An abnormal CSF flow pattern is seen in CM1 [77]. A spinal MRI is necessary to look for syringomyelia which may be seen in 40% of the patients, commonly located between the C4 and C6 levels [78]. Tonsillar ectopia may also be caused by disorders producing high and low CSF pressure, including mass lesions, which are distinct from a true Chiari malformation (Fig. 4.21).

Fig. 4.21 Arnold-Chiari type I and headache. Sagittal T2w image: caudal descent of cerebellar tonsils. Narrowing of subarachnoid space at craniocervical junction

4.3.2.4 Headache Attributed to Intracranial Infection

In cases of cerebral infections, these can be focal (i.e., abscess) or diffuse. In the latter situation, a distinction can be made between inflammation of the cerebral parenchyma (encephalitis) and cerebral membranes (meningitis).

The guiding symptoms of intracranial infection are headache and fever. Depending on the site and extent of the infection, additional neurological symptoms, including death, may occur.

Particular attention, however, should be paid to immune system-compromised and HIV-positive patients [79]. Intracranial pathology is found in cases of new-onset headache in up to 82% of these patients [80, 81]. Therefore cerebral imaging should be performed after new-onset headache or if existing symptoms change in type or intensity.

Meningitis is a clinical diagnosis supported by testing cerebrospinal fluid. The use of imaging therefore is to exclude contraindications for a lumbar puncture [82]. Performing non-enhanced CT is sufficient here. In cases of bacterial meningitis and in those with unfavorable progression of the disease, CT or MRI with contrast media should be performed (Fig. 4.22).

If encephalitis is suspected, an MRI should be performed. Inflammatory changes appear as hyperintense signal alterations in FLAIR images and in diffusion-weighted images can be distinguished earlier as hyperintense signal alteration. Administration of contrast agent is required, and contrast-enhanced images should be acquired on at least two planes.

4.3.2.5 Painful Cranial Neuropathies and Other Facial Pains

Glossopharyngeal Neuralgia

Glossopharyngeal neuralgia (GN) is an uncommon facial pain syndrome and is often misdiagnosed as trigeminal neuralgia. Generally, GN is

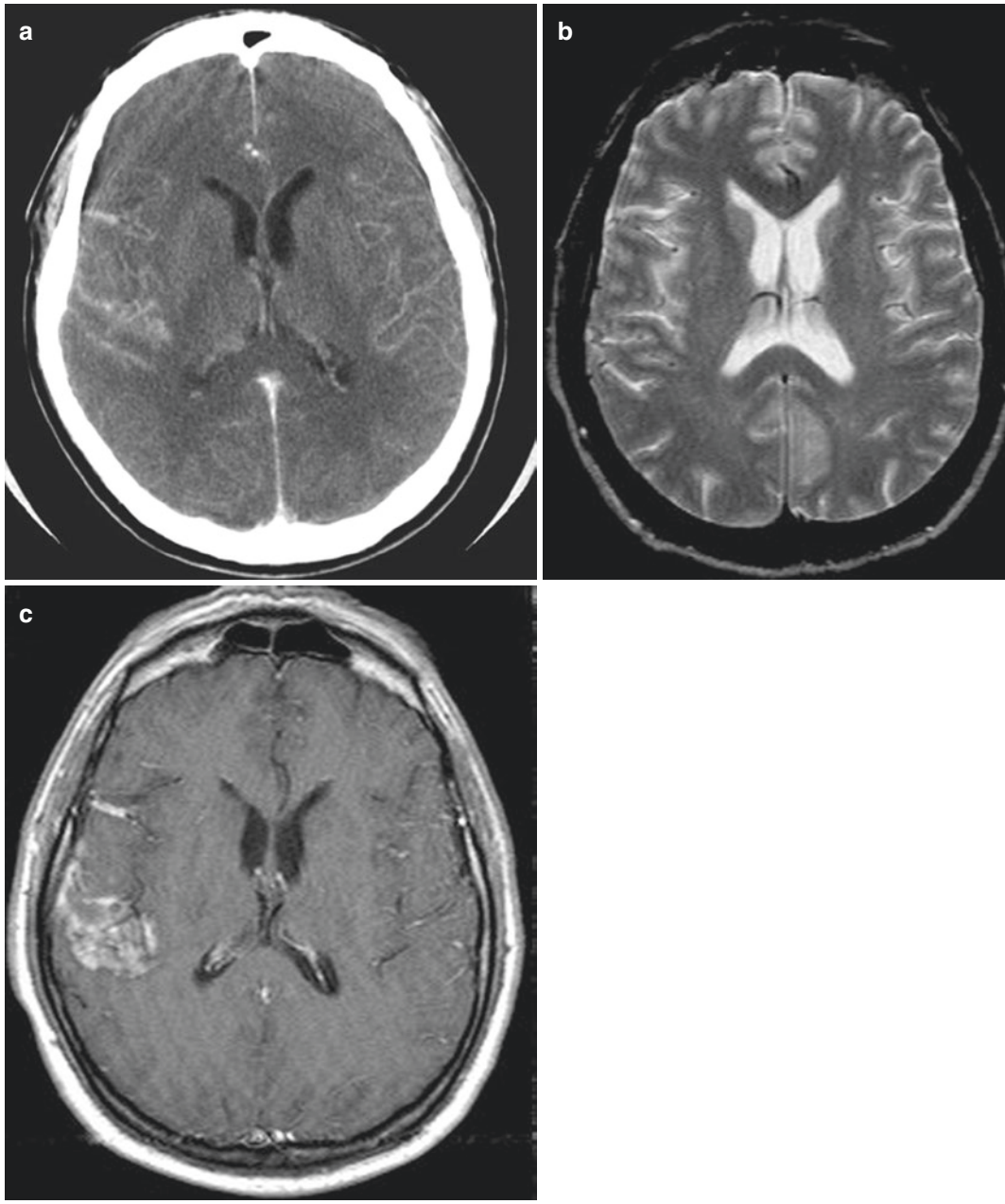

Fig. 4.22 TBC meningitis in patient with headache and subtle left hemiparesis. CT scan after CM (**a**), SE T2-weighted image (**b**), SE T1w image after CM (**c**). Meningeal thickening and enhancement at the level of right insula is demonstrated both in CT (**a**) and T1W image after contrast media administration (**c**). No clear pathologic sign is shown on T2w image (**b**)

caused by neurovascular compression, while trauma, neoplasms, infection, or an elongated styloid process represent only a minor percentage. Imaging of the neck is necessary to exclude a neoplasm of the hypopharynx, larynx, or piriform sinus or an elongated styloid process (Fig. 4.23). MRI is the exam of choice to rule out the presence of a neurovascular compression: the

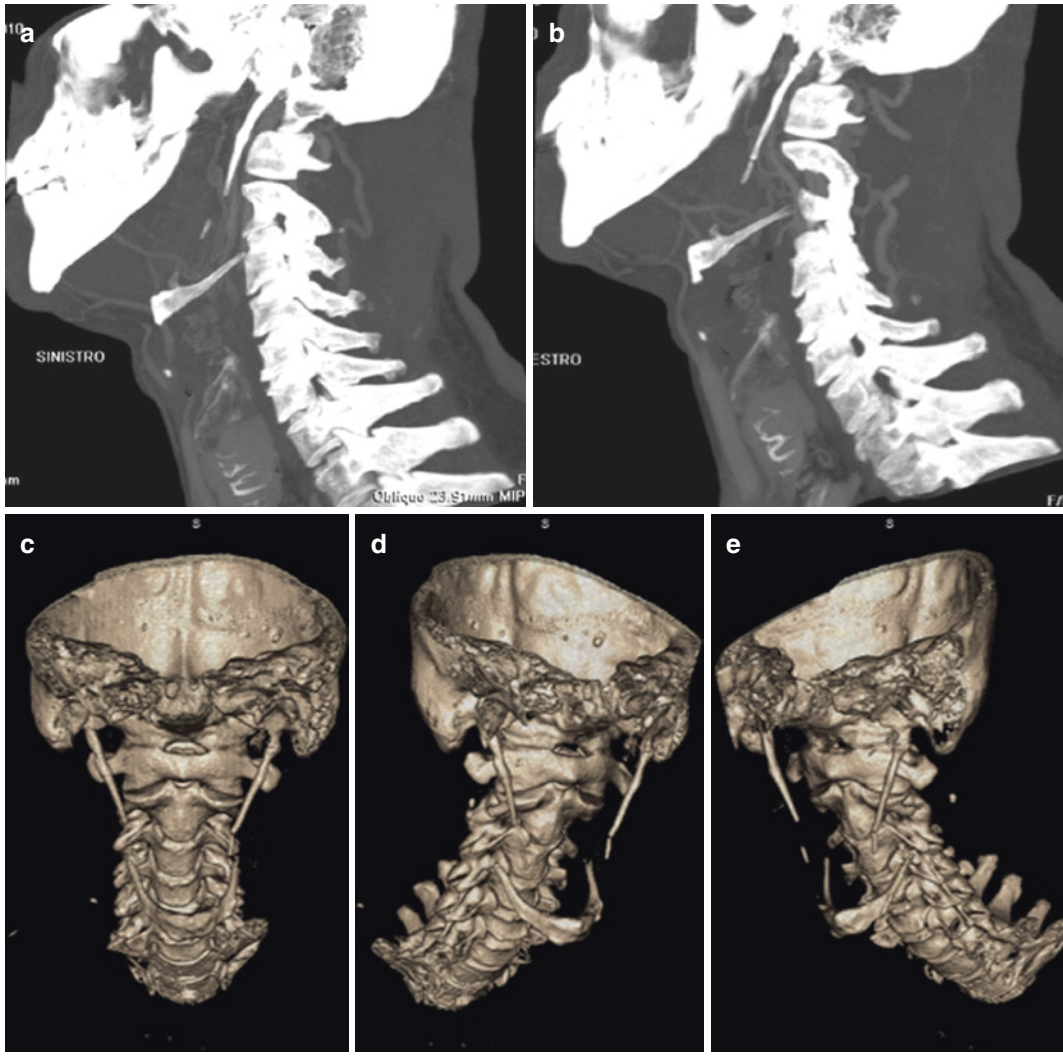

Fig. 4.23 Eagle syndrome in patient with parapharyngeal chronic pain. CT MIP sagittal (**a**, **b**) and 3D reconstruction (**c**–**e**) show an elongated styloid process on the left associated with calcification of stylohyoid ligament

combination of high-resolution 3D T2-weighted imaging with 3D time-of-flight angiography and 3D T1-weighted gadolinium-enhanced sequences is considered the standard of reference for the detection of neurovascular compression and can successfully guide neurosurgical treatment [83]. MRI allows precise assessment of the relationship between the IX nerve and the conflicting artery in the supraolivary fossette, which is the site of origin of the IX nerve; the posterior inferior cerebellar artery and less frequently the anterior inferior cerebellar artery are responsible for nerve compression [83, 84] (Fig. 4.24).

Tolosa-Hunt Syndrome

Tolosa-Hunt syndrome (THS) is a very rare disorder characterized by unilateral orbital pain associated with paresis of one or more of the third, fourth, and/or fifth cranial nerves. It is a benign condition caused by granulomatous inflammation in the cavernous sinus, superior orbital fissure, or both which resolve promptly after corticosteroid treatment [2, 85]. MRI is important to rule out other pathologies of the cavernous sinus such as neoplasms, infections, vascular abnormalities, and venous thrombosis as

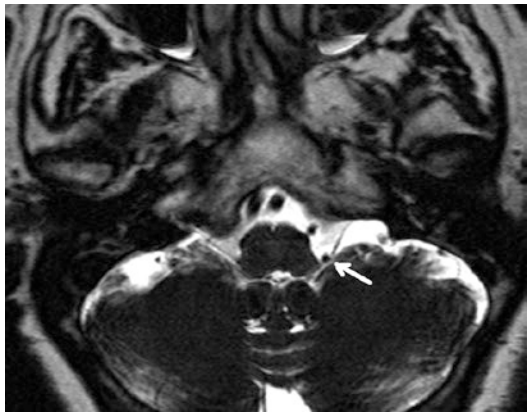

Fig. 4.24 Glossopharyngeal neuralgia—left pharyngeal pain. 3D TSE T2-weighted image: left glossopharyngeal nerve in contact with left PICA at supraolivary fossette (arrow)

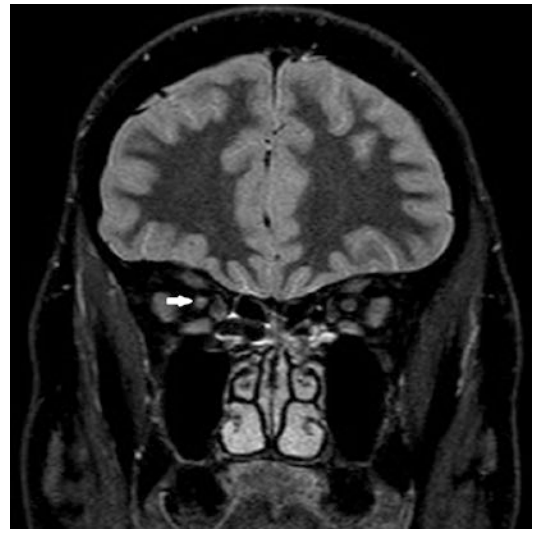

Fig. 4.25 Optic neuritis in patient with visual lost and orbital pain. Coronal STIR demonstrates hyperintensity of the right optic nerve

the cause of symptoms. Typical MRI findings in THS include enlargement of the cavernous sinus due to soft tissue extending through the superior orbital fissure into the orbital apex. The soft tissue lesion shows isointense signal intensity on T1w and iso-hypointense signal intensity on T2w sequences with enhancement after contrast media injection. The follow-up MRI after corticosteroid therapy shows resolution of radiological findings which supports the diagnosis and also identifies the relapse early [85–87].

Optic Neuritis

Optic neuritis (ON) is characterized by unilateral or bilateral pain localized in retro-orbital, orbital, frontal, and/or temporal regions, aggravated by eye movement and accompanied by impairment of central vision [2]. The optic nerve is not well characterized on conventional brain MRI sequences because of its small size and surrounding orbital fat; therefore an orbital MRI protocol is used, with T1 and T2 sequences obtained before and after gadolinium injection and with fat suppression sequences since the orbital portion of the optic nerve is surrounded by fat (Fig. 4.25). ON is a common presentation of multiple sclerosis (MS) in approximately 20% of patients: common imaging features in MS-ON are a short involvement of the optic nerves, often unilaterally [88, 89]. Otherwise, a unilateral or bilateral long involvement of the posterior aspects of the nerve and/or chiasma may suggest the presence of a neuromyelitis optica spectrum disorder (NMOSD), in accordance to other clinical, serological, and neuroimaging features [89]. A diagnosis of NMOSD should be kept in mind in more severe ON, usually involving optic nerves bilaterally, with positivity of serum anti-aquaporin 4 autoantibody (anti-AQP4 Ab) and in patients with associated acute transverse myelitis, mostly longitudinally extended (with three or more vertebral segments involved), with central cord involvement, cord expansion, and T1 hypointensity during the acute phase [89].

References

1. Douglas AC, Wippold FJ, Broderick DF, Aiken AH, Amin-Hanjani S, Brown DC, et al. ACR appropriateness criteria headache. J Am Coll Radiol. 2014;11(7):657–67.
2. Olesen J. The international classification of headache disorders, 3rd edition. Cephalagia. 2013;33(9):629–808.
3. Vetvik KG, MacGregor EA. Sex differences in the epidemiology, clinical features, and pathophysiology of migraine. Lancet Neurol. 2017;16(1):76–87.

4. Blau J. Migraine: clinical and research aspects. Baltimore: Johns Hopkins University Press; 1987. p. 695.
5. Schoenen J, Sándor PS. Headache with focal neurological signs or symptoms: a complicated differential diagnosis. Lancet Neurol. 2004;3(4):237–45.
6. Cooney BS, Grossman RI, Farber RE, Goin JE, Galetta SL. Frequency of magnetic resonance imaging abnormalities in patients with migraine. Headache. 1996;36(10):616–21.
7. Kamson DO, Illés Z, Aradi M, Orsi G, Perlaki G, Leél-Ssy E, et al. Volumetric comparisons of supratentorial white matter hyperintensities on FLAIR MRI in patients with migraine and multiple sclerosis. J Clin Neurosci. 2012;19(5):696–701.
8. Sher A, Gudmundsson L, Sigurdsson S, Ghambaryan A, Aspelund T, Eiriksdottir G, et al. Migraine headache in middle age and late-life brain infarcts: the age gene/environment susceptibility—Reykjavik study. JAMA. 2009;301(24):2563–70.
9. Kurth T, Mohamed S, Maillard P, Zhu Y-C, Chabriat H, Mazoyer B, et al. Headache, migraine, and structural brain lesions and function: population based epidemiology of vascular ageing-MRI study. BMJ. 2011;342:c7357.
10. Kruit MC, Van Buchem MA, Launer LJ, Terwindt GM, Ferrari MD. Migraine is associated with an increased risk of deep white matter lesions, subclinical posterior circulation infarcts and brain iron accumulation: the population-based MRI CAMERA study. Cephalalgia. 2010;30(2):129–36.
11. Uggetti C, Squarza S, Longaretti F, Galli A, Di Fiore P, Reganati PF, et al. Migraine with aura and white matter lesions: an MRI study. Neurol Sci. 2017;38:11–3.
12. Lin FY, Yang CY. Reversible splenial lesion of the corpus callosum in migraine with aura. Neurologist. 2011;17(3):157–9.
13. Sanchez Del Rio M, Bakker D, Wu O, Agosti R, Mitsikostas DD, Østergaard L, et al. Perfusion weighted imaging during migraine: spontaneous visual aura and headache. Cephalalgia. 1999;19(8):701–7.
14. Baron J. Stroke: imaging and differential diagnosis. J Neural Transm Suppl. 2002;63:19–36.
15. Cheng M, Wu Y, Tang S. Cerebral perfusion changes in hemiplegic migraine: illustrated by Tc-99m ECD brain perfusion scan. Clin Nucl Med. 2010;35(6):456–8.
16. Linn J, Freilinger T, Morhard D, Brückmann H, Straube A. Aphasic migraineous aura with left parietal hypoperfusion: a case report. Cephalalgia. 2007;27(7):850–3.
17. Relja G, Granato A, Ukmar M, Ferretti G, Antonello RM, Zorzon M. Persistent aura without infarction: description of the first case studied with both brain SPECT and perfusion MRI. Cephalalgia. 2005;25(1):56–9.
18. Yamada K, Harada M, Inoue N, Yoshida S, Morioka M, Kuratsu JI. Concurrent hemichorea and migrainous aura—a perfusion study on the basal ganglia using xenon-computed tomography. Mov Disord. 2008;23(3):425–9.
19. Kato Y, Araki N, Matsuda H, Ito Y, Suzuki C. Arterial spin-labeled MRI study of migraine attacks treated with rizatriptan. J Headache Pain. 2010;11(3):255–8.
20. Floery D, Vosko MR, Fellner FA, Fellner C, Ginthoer C, Gruber F, et al. Acute-onset migrainous aura mimicking acute stroke: MR perfusion imaging features. AJNR Am J Neuroradiol. 2012;33(8):1546–52.
21. Resnick S, Reyes-Iglesias Y, Carreras R, Villalobos E. Migraine with aura associated with reversible MRI abnormalities. Neurology. 2006;66(6):946–7.
22. Shah L, Rana S, Valeriano J, Scott TF. Reversible CT perfusion abnormalities in patient with migraine variant: a two phase process. Clin Neurol Neurosurg. 2013;115(6):830–2.
23. Hansen JM, Schytz HW, Larsen VA, Iversen HK, Ashina M. Hemiplegic migraine aura begins with cerebral hypoperfusion: imaging in the acute phase. Headache. 2011;51(8):1289–96.
24. Lykke Thomsen L, Kirchmann Eriksen M, Faerch Romer S, Andersen I, Ostergaard E, Keiding N, et al. An epidemiological survey of hemiplegic migraine. Cephalalgia. 2002;22:361–75.
25. Welch KM. Contemporary concepts of migraine pathogenesis. Neurology. 2003;61(8 Suppl 4):S2–8.
26. Cha YH, Millett D, Kane M, Jen J, Baloh R. Adult-onset hemiplegic migraine with cortical enhancement and oedema. Cephalalgia. 2007;27(10):1166–70.
27. Dreier JP, Jurkat-Rott K, Petzold GG, Tomkins O, Klingebiel R, Kopp UA, et al. Opening of the blood-brain barrier preceding cortical edema in a severe attack of FHM type II. Neurology. 2005;64(12):2145–7.
28. Pelzer N, Hoogeveen ES, Ferrari MD, Poll-The BT, Kruit MC, Terwindt GM. Brain atrophy following hemiplegic migraine attacks. Cephalalgia. 2017;38:1199.
29. Codeluppi L, Bonifacio G, Chiari A, Ariatti A, Nichelli PF. Optic nerve involvement in retinal migraine. Headache. 2015;55(4):562–4.
30. Bigal ME, Serrano D, Buse D, Scher A, Stewart WF, Lipton RB. Acute migraine medications and evolution from episodic to chronic migraine: a longitudinal population-based study. Headache. 2008;48(8):1157–68.
31. Scher AI, Stewart WF, Ricci JA, Lipton RB. Factors associated with the onset and remission of chronic daily headache in a population-based study. Pain. 2003;106(1-2):81–9.
32. Neeb L, Bastian K, Villringer K, Israel H, Reuter U, Fiebach JB. Structural gray matter alterations in chronic migraine: implications for a progressive disease? Headache. 2017;57(3):400–16.
33. Kittner SJ, Stern BJ, Wozniak M, Buchholz DW, Earley CJ, Feeser BR, et al. Cerebral infarction in young adults: the Baltimore-Washington Cooperative Young Stroke Study. Neurology. 1998;50:890–4.
34. Sacquegna T, Baldrati A, Lamieri C, Guttmann S, De Carolis P, Lugaresi E, et al. Ischemic stroke in young adults: the relevance of migrainous infarction. Cephalalgia. 1989;9(4):255–8.

35. Arboix A, Massons J, García-Eroles L, Oliveres M, Balcells M, Targa C. Migrainous cerebral infarction in the Sagrat Cor Hospital of Barcelona stroke registry. Cephalalgia. 2003;23(5):389–94.
36. Swartz RH, Kern RZ. Migraine is associated with magnetic resonance imaging white matter abnormalities: a meta-analysis. Arch Neurol. 2004;61(9):1366–8.
37. Kruit MC. Migraine as a risk factor for subclinical brain lesions. JAMA. 2004;291(4):427.
38. Gass A, Ay H, Szabo K, Koroshetz WJ. Diffusion-weighted MRI for the "small stuff": the details of acute cerebral ischaemia. Lancet Neurol. 2004;3(1):39–45.
39. Fiebach J, Jansen O, Schellinger P, Knauth M, Hartmann M, Heiland S, et al. Comparison of CT with diffusion-weighted MRI in patients with hyperacute stroke. Neuroradiology. 2001;43(8):628–32.
40. Ay H, Buonanno FS, Rordorf G, Schaefer PW, Schwamm LH, Wu O, et al. Normal diffusion-weighted MRI during stroke-like deficits. Neurology. 1999;52(9):1784–92.
41. Mitsikostas DD, Ashina M, Craven A, Diener HC, Goadsby PJ, Ferrari MD, et al. European headache federation consensus on technical investigation for primary headache disorders. J Headache Pain. 2015;17(1):5.
42. Wang P, Du H, Chen N, Guo J, Gong Q, Zhang J, et al. Regional homogeneity abnormalities in patients with tensiontype headache: a resting-state fMRI study. Neurosci Bull. 2014;30(6):949–55.
43. Chen B, He Y, Xia L, Guo L-L, Zheng J-L. Cortical plasticity between the pain and pain-free phases in patients with episodic tension-type headache. J Headache Pain. 2016;17(1):105.
44. Holle D, Obermann M. The role of neuroimaging in the diagnosis of headache disorders. Ther Adv Neurol Disord. 2013;6:369–74.
45. de Coo IF, Wilbrink LA, Haan J. Symptomatic trigeminal autonomic cephalalgias. Curr Pain Headache Rep. 2015;19(8):39.
46. May A. New insights into headache: an update on functional and structural imaging findings. Nat Rev Neurol. 2009;5(4):199–209.
47. Iacovelli E, Coppola G, Tinelli E, Pierelli F, Bianco F. Neuroimaging in cluster headache and other trigeminal autonomic cephalalgias. J Headache Pain. 2012;13(1):11–20.
48. Naegel S, Holle D, Obermann M. Structural imaging in cluster headache. Curr Pain Headache Rep. 2014;18(5):415.
49. Chaudhry P, Friedman DI. Neuroimaging in secondary headache disorders. Curr Pain Headache Rep. 2015;19(7):1–11.
50. Seifert CL, Schönbach EM, Magon S, Gross E, Zimmer C, Förschler A, et al. Headache in acute ischaemic stroke: a lesion mapping study. Brain. 2016;139(1):217–26.
51. Chen PK, Chiu PY, Tsai IJ, Tseng HP, Chen JR, Yeh SJ, et al. Onset headache predicts good outcome in patients with first-ever ischemic stroke. Stroke. 2013;44(7):1852–8.
52. Verdelho A, Madureira S, Ferro JM, Basile AM, Chabriat H, Erkinjuntti T, et al. Differential impact of cerebral white matter changes, diabetes, hypertension and stroke on cognitive performance among non-disabled elderly. The LADIS study. J Neurol Neurosurg Psychiatry. 2007;78(12):1325–30.
53. Seifert CL, Schönbach EM, Zimmer C, Förschler A, Tölle TR, Feurer R, et al. Association of clinical headache features with stroke location: an MRI voxel-based symptom lesion mapping study. Cephalalgia. 2016;38:283.
54. Mortimer AM, Bradley MD, Stoodley NG, Renowden SA. Thunderclap headache: diagnostic considerations and neuroimaging features. Clin Radiol. 2013;68(3):101–13.
55. De Oliveira Manoel AL, Mansur A, Murphy A, Turkel-Parrella D, Macdonald M, Macdonald RL, et al. Aneurysmal subarachnoid haemorrhage from a neuroimaging perspective. Crit Care. 2014;18(6):557.
56. Li M-H, Li Y, Gu B, Cheng Y, Wang W, Tan H, et al. Accurate diagnosis of small cerebral aneurysms ≤5 mm in diameter with 3.0-T MR angiography. Radiology. 2014;271(2):553–60.
57. Heit JJ, Iv M, Wintermark M. Imaging of intracranial hemorrhage. J Stroke. 2017;19(1):11–27.
58. Lester MS, Liu BP. Imaging in the evaluation of headache. Med Clin North Am. 2013;97(2):243–65.
59. Provenzale JM, Sarikaya B. Comparison of test performance characteristics of MRI, MR angiography, and CT angiography in the diagnosis of carotid and vertebral artery dissection: a review of the medical literature. AJR Am J Roentgenol. 2009;193(4):1167–74.
60. Sadigh G, Mullins ME, Saindane AM. Diagnostic performance of MRI sequences for evaluation of dural venous sinus thrombosis. Am J Roentgenol. 2016;206(6):1298–306.
61. Sari S, Verim S, Hamcan S, Battal B, Akgun V, Akgun H, et al. MRI diagnosis of dural sinus - cortical venous thrombosis: immediate post-contrast 3D GRE T1-weighted imaging versus unenhanced MR venography and conventional MR sequences. Clin Neurol Neurosurg. 2015;134:44–54.
62. Kang JH, Yun TJ, Yoo RE, Yoon BW, Lee AL, Kang KM, et al. Bright sinus appearance on arterial spin labeling MR imaging AIDS to identify cerebral venous thrombosis. Medicine (Baltimore). 2017;96(41):e8244.
63. Velez A, McKinney JS. Reversible cerebral vasoconstriction syndrome: a review of recent research. Curr Neurol Neurosci Rep. 2013;13(1):319.
64. Ioannidis I, Nasis N, Agianniotaki E, Katsouda E, Andreou A. Reversible cerebral vasoconstriction syndrome: treatment with multiple sessions of intra-arterial nimodipine and angioplasty. Interv Neuroradiol. 2012;18(3):297–302.
65. Komatsu T, Kimura T, Yagishita A, Takahashi K, Koide R. A case of reversible cerebral vasoconstriction syndrome presenting with recurrent neurological deficits: evaluation using noninvasive arterial spin labeling MRI. Clin Neurol Neurosurg. 2014;126:96–8.

66. Di Donato I, Bianchi S, De Stefano N, Dichgans M, Dotti MT, Duering M, et al. Cerebral Autosomal Dominant Arteriopathy with Subcortical Infarcts and Leukoencephalopathy (CADASIL) as a model of small vessel disease: update on clinical, diagnostic, and management aspects. BMC Med. 2017;15(1):41.
67. Zhu S, Nahas SJ. CADASIL: imaging characteristics and clinical correlation. Curr Pain Headache Rep. 2016;20(10):57.
68. Viswanathan A, Godin O, Jouvent E, O'Sullivan M, Gschwendtner A, Peters N, et al. Impact of MRI markers in subcortical vascular dementia: a multi-modal analysis in CADASIL. Neurobiol Aging. 2010;31(9):1629–36.
69. Mascalchi M, Pantoni L, Giannelli M, Valenti R, Bianchi A, Pracucci G, et al. Diffusion tensor imaging to map brain microstructural changes in CADASIL. J Neuroimaging. 2017;27(1):85–91.
70. Aslan K, Gunbey HP, Tomak L, Ozmen Z, Incesu L. Magnetic resonance imaging of intracranial hypotension. J Comput Assist Tomogr. 2017;0(0):1.
71. Haritanti A, Karacostas D, Drevelengas A, Kanellopoulos V, Paraskevopoulou E, Lefkopoulos A, et al. Spontaneous intracranial hypotension. Clinical and neuroimaging findings in six cases with literature review. Eur J Radiol. 2009;69(2):253–9. https://doi.org/10.1016/j.ejrad.2007.10.013.
72. Langner S, Kirsch M. Radiological diagnosis and differential diagnosis of headache. RöFo. 2015;187(10):879–91.
73. Schankin CJ, Ferrari U, Reinisch VM, Birnbaum T, Goldbrunner R, Straube A. Characteristics of brain tumour-associated headache. Cephalalgia. 2007;27(8):904–11.
74. Osborn AG, Preece MT. Intracranial cysts: radiologic-pathologic correlation and imaging approach. Radiology. 2006;239(3):650–64.
75. Urso JA, Ross GJ, Parker RK, Patrizi JD, Stewart B. Colloid cyst of the third ventricle: radiologic-pathologic correlation. J Comput Assist Tomogr. 1998;22(4):524–7.
76. Amer TA, El-Shmam OM. Chiari malformation type I: a new MRI classification. Magn Reson Imaging. 1997;15(4):397–403.
77. Hofkes SK, Iskandar BJ, Turski PA, Gentry LR, McCue JB, Haughton VM. Differentiation between symptomatic Chiari I malformation and asymptomatic tonsilar ectopia by using cerebrospinal fluid flow imaging: initial estimate of imaging accuracy. Radiology. 2007;245(2):532–40.
78. Elster AD, Chen MY. Chiari I malformations: clinical and radiologic reappraisal. Radiology. 1992;183(2):347–53.
79. Krope K, Speil A, Pantazis G, Nägele T, Horger M. Wertigkeit der MRT in der Diagnostik primärer und sekundärer zerebraler Infektionen. RöFo. 2013;185(6):539–45.
80. Edlow JA, Panagos PD, Godwin SA, Thomas TL, Decker WW. Clinical policy: critical issues in the evaluation and management of adult patients presenting to the emergency department with acute headache. Ann Emerg Med. 2008;52(4):407–36.
81. Joshi SG, Cho TA. Pathophysiological mechanisms of headache in patients with HIV. Headache. 2014;54(5):946–50.
82. van Crevel H, Hijdra A, de Gans J. Lumbar puncture and the risk of herniation: when should we first perform CT? J Neurol. 2002;249(2):129–37.
83. Haller S, Etienne L, Kövari E, Varoquaux AD, Urbach H, Becker M. Imaging of neurovascular compression syndromes: trigeminal neuralgia, hemifacial spasm, vestibular paroxysmia, and glossopharyngeal neuralgia. AJNR Am J Neuroradiol. 2016;37(8):1384–92.
84. Singh P, Trikha A, Kaur M. An uncommonly common: glossopharyngeal neuralgia. Ann Indian Acad Neurol. 2013;16(1):1.
85. Arshad A, Nabi S, Panhwar MS, Rahil A. Tolosa-Hunt syndrome: an arcane pathology of cavernous venous sinus. BMJ Case Rep. 2015;2015:bcr2015210646.
86. Sánchez Vallejo R, Lopez-Rueda A, Olarte AM, San Roman L. MRI findings in Tolosa-Hunt syndrome (THS). BMJ Case Rep. 2014;2014:bcr2014206629.
87. Wani NA, Jehangir M, Lone PA. Tolosa-Hunt syndrome demonstrated by constructive interference steady state magnetic resonance imaging. J Ophthalmic Vis Res. 2017;12(1):106–9.
88. Zabad R, Stewart R, Healey K. Pattern recognition of the multiple sclerosis syndrome. Brain Sci. 2017;7(11):138.
89. Whittam D, Wilson M, Hamid S, Keir G, Bhojak M, Jacob A. What's new in neuromyelitis optica? A short review for the clinical neurologist. J Neurol. 2017;264(11):2330–44.